The Company of Biologists

RESEARCH ARTICLE

The Rho guanine nucleotide exchange factor Trio is required for neural crest cell migration and interacts with Dishevelled

Marie-Claire Kratzer[1,2,*], Sarah F. S. Becker[3,*], Anita Grund[1], Anne Merks[4], Jakub Harnoš[5], Vítězslav Bryja[5,6], Klaudia Giehl[7], Jubin Kashef[8,‡] and Annette Borchers[1,2,‡]

ABSTRACT

Directional migration during embryogenesis and tumor progression faces the challenge that numerous external signals need to converge to precisely control cell movement. The Rho guanine exchange factor (GEF) Trio is especially well suited to relay signals, as it features distinct catalytic domains to activate Rho GTPases. Here, we show that Trio is required for *Xenopus* cranial neural crest (NC) cell migration and cartilage formation. Trio cell-autonomously controls protrusion formation of NC cells and Trio morphant NC cells show a blebbing phenotype. Interestingly, the Trio GEF2 domain is sufficient to rescue protrusion formation and migration of Trio morphant NC cells. We show that this domain interacts with the DEP/C-terminus of Dishevelled (DVL). DVL – but not a deletion construct lacking the DEP domain – is able to rescue protrusion formation and migration of Trio morphant NC cells. This is likely mediated by activation of Rac1, as we find that DVL rescues Rac1 activity in Trio morphant embryos. Thus, our data provide evidence for a novel signaling pathway, whereby Trio controls protrusion formation of cranial NC cells by interacting with DVL to activate Rac1.

KEY WORDS: GEF Trio, Neural crest cell migration, *Xenopus*, Dishevelled, Rho GTPases, Cadherin-11

INTRODUCTION

Directed cell migration controls a plethora of crucial events in embryonic development and adult homeostasis, including morphogenetic cell movements, wound healing and immune function, as well as tumor cell migration. Neural crest (NC) cells are embryonic multipotent cells, which have been likened to cancer metastasis and provide an excellent example for analyzing the molecular mechanisms that control cell migration (Theveneau and Mayor, 2011). NC cells migrate over long distances throughout the embryo where they contribute to the formation of various tissue types, including neurons, glia, cartilage, smooth muscle and pigment cells. Thus, NC cell migration needs to be precisely controlled, as defects can lead to severe congenital malformations, including craniofacial and heart defects, hearing loss and mental retardation (Trainor, 2014).

Collective chemotaxis, repellent guidance cues along with dynamic cell-matrix and cell-cell interactions synergize to regulate the directional migration of NC cells (Shellard and Mayor, 2016; Szabó and Mayor, 2018). Migrating cells extend protrusions in the form of lamellipodia and filopodia in the direction of migration, while they retract them at the trailing edge. Cell migration is directed by attractive signals such as Sdf1 or VEGFA (McLennan et al., 2010; Theveneau et al., 2013) as well as repulsive cues like semaphorins and ephrins (Gammill et al., 2007, 2006; Smith et al., 1997). These, sometimes contradictory, signals have to be integrated to allow for directional migration (Bajanca et al., 2019). Although attractive and repulsive cues originate from the surrounding tissue, including the placodes, NC cells also exchange information via transient cell-cell contacts. For example, they show contact inhibition of locomotion, a phenomenon whereby cells change their direction upon cell-cell contact formation (Abercrombie and Heaysman, 1953; Roycroft and Mayor, 2018). In the past decade, contact inhibition of locomotion has been shown to be crucial for directional migration of cranial NC cells (Carmona-Fontaine et al., 2008; Matthews et al., 2008; Theveneau et al., 2010, 2013). A number of molecular regulators of cranial NC migration have been identified, including: adhesion molecules, such as N-cadherin and cadherin-11; effectors of Wnt planar cell polarity (PCP) signaling, such as Frizzled 7 (Fz7) and Dishevelled (DVL); and the cell polarity protein Par3 (Becker et al., 2013; Carmona-Fontaine et al., 2008; Moore et al., 2013; Theveneau et al., 2010). These molecules synergize to control the activity of small GTPases of the Rho family, which then leads to retraction of protrusions at the cell-cell contact site and formation of new protrusions in the direction of migration.

The complex signaling network affecting directional migration of NC cells converges at the level of small GTPases of the Rho family. RhoA, Rac1 and Cdc42 are crucial regulators of cellular morphology and locomotion, and are activated by binding of GTP. The exchange of GDP to GTP is controlled by guanine nucleotide exchange factors (GEFs), which determine the temporal and spatial activity of Rho GTPases (Nguyen et al., 2018). The Rho GEF Trio is especially well suited to dynamically control protrusive activity of cranial NC cells. The protein was named Trio as it features two GEF domains of distinct specificity as well as a serine/threonine kinase domain (Debant et al., 1996). The N-terminal GEF1 domain activates Rac1 and RhoG, while the C-terminal GEF2 domain specifically acts on RhoA (Bellanger et al., 1998;

[1]Philipps-Universität Marburg, Faculty of Biology, Molecular Embryology, 35043 Marburg, Germany. [2]DFG Research Training Group, Membrane Plasticity in Tissue Development and Remodeling, GRK 2213, Philipps-Universität Marburg, Marburg, Germany. [3]Department of Development and Stem Cells, Institut de Génétique et de Biologie Moléculaire et Cellulaire, CNRS UMR 7104/INSERM U1258, Université de Strasbourg, F-67400 Illkirch, CU Strasbourg, France. [4]Max Delbrück Center for Molecular Medicine in the Helmholtz Association, 13125 Berlin, Germany. [5]Department of Experimental Biology, Faculty of Science, Masaryk University, Brno 62500, Czech Republic. [6]Department of Cytokinetics, Institute of Biophysics of the Academy of Sciences of the Czech Republic v.v.i., Brno 61265, Czech Republic. [7]Signal Transduction of Cellular Motility, Internal Medicine V, Justus Liebig University Giessen, D-35392 Giessen, Germany. [8]Institute for Photon Science and Synchrotron Radiation, Karlsruhe Institute of Technology (KIT), 76344 Eggenstein-Leopoldshafen, Germany.
*These authors contributed equally to this work

‡Authors for correspondence (borchers@uni-marburg.de; jubinkashef@gmx.de)

J.H., 0000-0002-0752-9260; V.B., 0000-0002-9136-5085; A.B., 0000-0002-2524-5384

DEVELOPMENT

Blangy et al., 2000; Debant et al., 1996). Furthermore, Trio exhibits an N-terminal putative lipid-transfer SEC14 domain, a variable number of spectrin-like domains, two Src-homology 3 domains, one immunoglobulin-like domain, and a C-terminal serine/ threonine kinase domain. Thus, Trio is well suited to function as a signal integrator of various molecular stimuli during development and disease. Indeed, Trio has been shown to have an evolutionarily conserved role in the development of the nervous system and its expression is upregulated in different tumors (reviewed by Schmidt and Debant, 2014). Furthermore, *de novo* mutations of Trio have been identified in individuals with a combination of neurodevelopmental, skeletal and craniofacial abnormalities (Ba et al., 2016; Pengelly et al., 2016), the last being suggestive of defects in the development of the neural crest. In fact, a function of Trio in the control of NC migration is supported by its expression in migrating *Xenopus* cranial NC cells (Kratzer et al., 2019). Indeed, a number of molecules that interact with Trio and control cell migration have been identified (reviewed by Schmidt and Debant, 2014; van Rijssel and van Buul, 2012), including focal adhesion kinase, cell-adhesion molecules of the cadherin family and proteins involved in cytoskeletal dynamics (Backer et al., 2007; Bellanger et al., 2000; Charrasse et al., 2007; Kashef et al., 2009; Medley et al., 2003; Timmerman et al., 2015; Vanderzalm et al., 2009; Yano et al., 2011). Moreover, Trio interacts with Cadherin-11 (Cad11) and can rescue protrusion formation and migration of cranial NC cells in Cad11 morphant embryos (Kashef et al., 2009; Li et al., 2011). Recently, Trio has been shown to interact with the polarity protein Par3 (Landin Malt et al., 2019; Moore et al., 2013), which is required for contact inhibition of locomotion during NC migration (Moore et al., 2013). At NC cell-cell contacts, Par3 promotes microtubule catastrophe, likely by inhibiting Trio-dependent activation of Rac1. As Trio interacts with Cad11, which is localized in NC cell protrusions as well as at NC cell-cell contacts (Kashef et al., 2009), Trio may likely exert additional functions in the control of NC migration. Thus, in this study we further dissected the role of this unique molecule in NC migration.

RESULTS
Trio is required for cranial NC cell migration and formation of craniofacial cartilage

First, we revisited Trio function in *Xenopus* NC cell migration by repeating previously published loss-of-function experiments (Moore et al., 2013). Trio morpholino antisense oligonucleotides (Trio MO) were targeted to cranial NC cells and NC development was analyzed by *in situ* hybridization for AP-2α, a known marker of cranial NC cells. As expected Trio loss of function severely impaired NC migration (Fig. 1A), whereas neither injection of the Trio MO nor a control MO (Co MO) affected the induction of AP-2α-positive NC cells (Fig. S1). Compared with the uninjected side of the embryo, the Trio MO-injected side showed severe defects in NC cell migration, while NC cell migration was not affected by injection of a control MO. This effect is specific to Trio loss of function as the cranial NC migration defects could be rescued by co-injection of a human Trio DNA, which lacks the sequence targeted by the Trio MO (Fig. 1A,B; Moore et al., 2013). Overexpression of Trio in control MO-injected embryos did not cause NC migration defects (data not shown). These results were further verified using a second Trio MO: Trio MO2 (Fig. 1A,B). In addition, we confirmed that both Trio MO inhibited embryonic Trio expression (Fig. 1C,D). Furthermore, to test whether Trio function is required in NC cells, we performed transplantation experiments. Transplants injected with control MO exhibited directional

migration towards the pharyngeal pouches (Fig. 1E,F). In contrast, the migration of transplants from Trio morphants was severely inhibited (Fig. 1E,F). These defects were rescued by co-injection of Trio, which restored the directional migration of cranial NC cells.

One of the major derivatives of cranial NC cells is the craniofacial cartilage. Therefore, we asked whether Trio knockdown affects craniofacial morphogenesis as a consequence of disturbed NC cell migration. Indeed, Trio morphant embryos displayed severe defects in head cartilage morphology, as shown by Alcian Blue staining (Fig. 1G). Whereas control MO injected embryos exhibited bilateral symmetric cartilage structures, Trio MO injection led to loss of Meckel's cartilage and reduced posterior cartilage structures. Co-injection of human Trio rescued the craniofacial phenotype (Fig. 1G). Taken together, these results demonstrate that Trio is required for cranial NC cell migration in a cell-autonomous manner and is important for the formation of cartilage head structures in *Xenopus* embryos.

Trio is required for filopodia and lamellipodia formation

In order to identify the cellular function of Trio, we performed *in vitro* time-lapse analysis of cranial NC cells explanted on fibronectin. Wild-type NC cells injected with GAP43-GFP to mark the membrane (green) exhibited intense protrusive activity by forming filopodia and lamellipodia (Fig. 2A; Movie 1). In contrast, NC cells from Trio morphants completely lost their ability to form cell protrusions and showed membrane blebbing instead (Fig. 2A; Movie 2). Co-expression of human Trio DNA in morphant NC cells restored cell protrusion formation (Fig. 2A; Movie 3). This is also reflected by a significant increase in cell circularity of morphant NC cells compared with controls, which is rescued by co-expression of human Trio (Fig. 2B).

As Trio is an exchange factor for Rac1 and RhoA (Bellanger et al., 1998; Blangy et al., 2000; Debant et al., 1996), which modulate F-actin dynamics that are important for filopodia and lamellipodia formation (Hall, 1998), we co-injected NC cells with lifeact-mCherry to visualize F-actin dynamics. In wild-type NC cells, F-actin was enriched in stress fibers and in cell protrusions at the leading edge (Fig. 2C). In contrast, in Trio morphant NC cells, F-actin staining appeared more diffuse, but was also detected outlining the cell cortex of the blebs, consistent with a function in stabilization of the extending bleb (reviewed by Fackler and Grosse, 2008) (Fig. 2C, yellow arrowheads). In contrast, NC morphant cells co-injected with human Trio displayed the same cellular morphology as wild-type NC cells (Fig. 2C). Thus, Trio seems to be crucial for filopodia and lamellipodia formation in NC cells. This is further supported by Trio localization in explanted NC cells. NC cells expressing Trio-GFP together with GAP43-mCherry, showed Trio localization at the plasma membrane at cell-cell contacts, as well as cell protrusions (Fig. 2D, arrows). Taken together, the Trio loss-of-function phenotype as well as its subcellular localization supports a requirement of Trio for cell protrusion formation that is essential for cranial NC migration.

Rac1 and RhoA act downstream of Trio in the control of cranial NC cell migration

As cell protrusion formation depends on the activity of small GTPases of the Rho family, like Rac1, RhoA and Cdc42 (Jaffe and Hall, 2005), and as Trio is a known GEF, these small GTPases likely act downstream of Trio. Therefore, we first analyzed whether Trio activates Rac1, a known activator of cell protrusions (Hall, 1998). Rac1 pull-down assays were performed using *Xenopus* embryos that
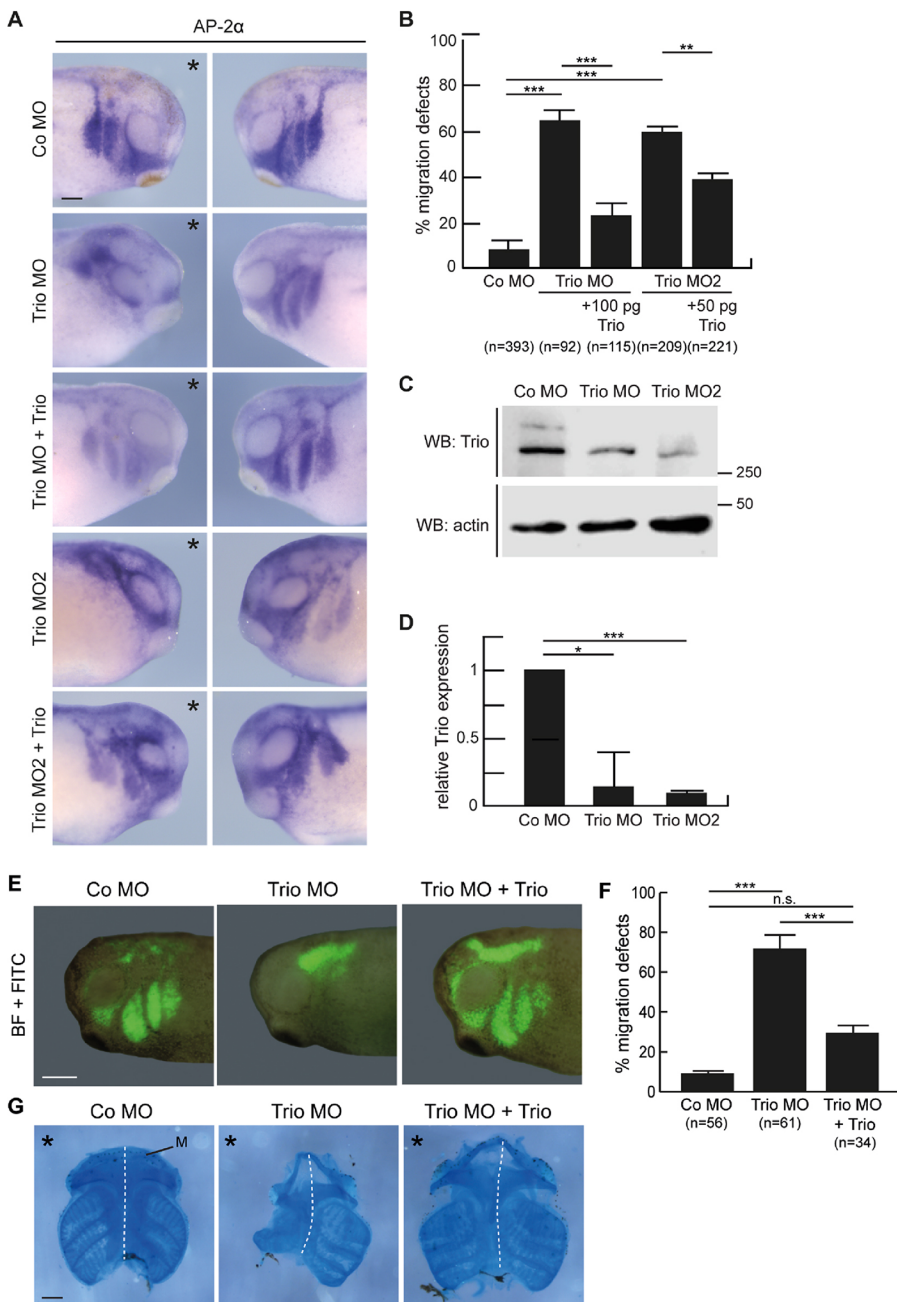
Fig. 1. Trio loss of function affects cranial NC migration and cartilage formation. (A) *Xenopus* embryos were injected with 5 ng control MO (Co MO), 5 ng Trio MO or 5 ng Trio MO2 into one animal dorsal blastomere of 8-cell stage embryos. NC cell migration was analyzed at stage 26 by AP-2α *in situ* hybridization. Co-injection of 100 pg Trio DNA with Trio MO or 50 pg Trio DNA with Trio MO2 could restore NC cell migration. Asterisks mark the injected side. Scale bar: 200 μm. (B) Graph summarizing the percentage of embryos with NC cell migration defects in at least three independent experiments. Number of embryos (*n*) are indicated for each column. Data are mean±s.e.m. (C) Lysates of stage 12 embryos injected with 5 ng control MO (Co MO), 5 ng Trio MO or 5 ng Trio MO2. Western blot analysis of Trio expression; actin was used as a loading control. WB: western blotting. Molecular weights (kDa) are indicated on the right. (D) Quantification of Trio expression normalized to actin of three independent experiments. Data are mean±s.e.m. (E) Embryos were injected as indicated in A and FITC-dextran (green fluorescence) was co-injected as a lineage tracer. NC cells were transplanted at premigratory NC stages; transplanted embryos were imaged at stage 26. Merge of bright-field (BF) and FITC channels. Scale bar: 250 μm. (F) Graph summarizing the percentage of transplanted embryos with NC cell migration defects. Number of embryos (*n*) are indicated for each column. Data are mean±s.e.m. (G) Alcian Blue staining of dissected cartilage structures of tadpole stage embryos injected as described in A. Asterisks mark the injected side. M: Meckel's cartilage. Dashed line indicates the midline of the cartilage structure. Scale bar: 250 μm. ***$P<0.005$, **$P<0.01$, *$P<0.05$; n.s., not significant (one-way ANOVA).

were injected with full-length Trio, the Trio GEF1 or GEF2 domain, or Trio MO (Fig. 3A,B). Overexpression of Trio and GEF1 significantly increased Rac1-GTP; however, the GEF2 domain also led to a minor increase in Rac1 activity. In contrast, knockdown of Trio by MO injection significantly decreased Rac1 activity (Fig. 3A,B).

Next, to elucidate whether the small GTPases of the Rho family act downstream of Trio, we tested whether constitutively active forms of RhoA, Rac1 or Cdc42 are, per se, able to rescue the Trio morphant phenotype. Embryos were injected with Trio MO in combination with either constitutive active RhoA, Rac1 or Cdc42, and NC cell migration was analyzed in whole embryos using AP-2α *in situ* hybridization (Fig. 3C,D). While RhoA and Rac1 alone, or in combination, were able to rescue the Trio morphant phenotype, Cdc42 did not. Overexpression of constitutive active RhoA, Rac1 or

Cdc42 alone did not cause craniofacial defects (data not shown). Similar results were also obtained by analyzing protrusion formation in explants co-injected with *GAP43-GFP* and *H2B-mcherry* RNA to visualize the plasma membrane or nucleus, respectively. Co-injection of RhoA and Rac1 restored protrusion formation in Trio morphant NC cells, while Cdc42-co-injected cells showed a blebbing phenotype (Fig. 3E). Taken together, these data indicate that RhoA and Rac1, but not Cdc42, act downstream of Trio in protrusion formation and migration of cranial NC cells.

NC cell migration and cell protrusion formation depends on the GEF2 domain of Trio

The Rho GEF Trio has two GEF domains: the N-terminal GEF1 domain mediates the exchange of GDP to GTP of Rac1 and RhoG, whereas the C-terminal GEF2 domain activates RhoA (Bellanger
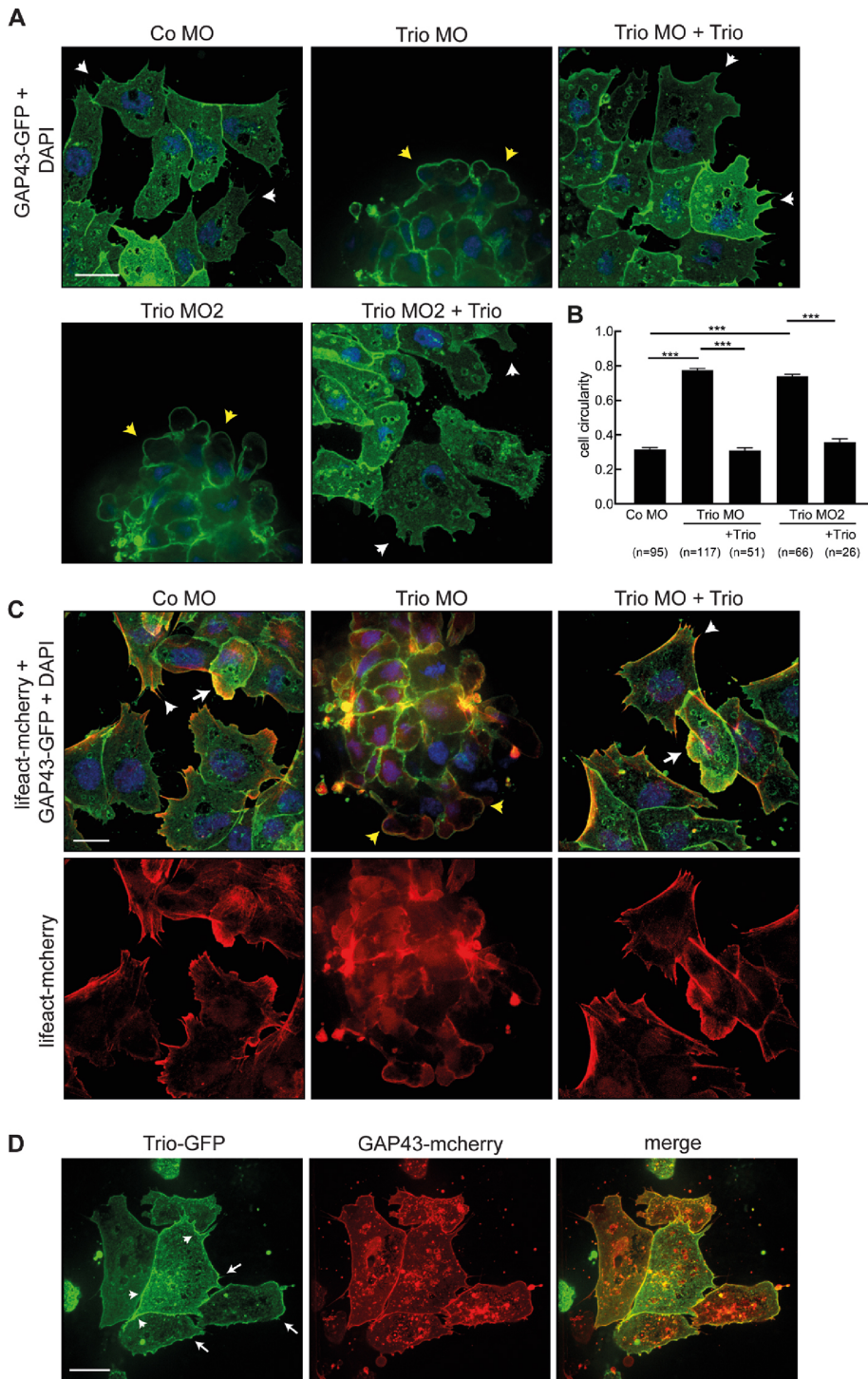
Fig. 2. Trio knockdown inhibits protrusion formation in cranial NC cells. (A) Embryos were injected with 5 ng control MO (Co MO), 5 ng Trio MO or 5 ng Trio MO2 in combination with 150 pg *GAP43-GFP* (to mark the membrane) into one animal dorsal blastomere of 8-cell stage embryos. NC cells were explanted at stage 16, cultured for 5 h, and fixed and stained with DAPI (blue). Co-injection of 100 pg Trio DNA with Trio MO or 50 pg Trio DNA with Trio MO2 restored NC cell protrusion formation. Yellow arrowheads mark cell blebs; white arrowheads indicate cell protrusions. (B) Averaged cell circularity of injected NC cells. Numbers of cells (*n*) are indicated for each column. Data are mean±s.e.m. ***P<0.001 (one-way ANOVA). (C) Explants of embryos injected at the 8-cell stage with 8 ng Co MO, 8 ng Trio MO or 8 ng Trio MO in combination with 10 pg Trio DNA. 300 pg *lifeact-mcherry* RNA (red) was co-injected to visualize the actin cytoskeleton, 500 pg *GAP43-GFP* RNA (green) to mark the membrane. DAPI staining (blue) marks the nuclei. The lower panel shows only the actin (lifeact-mCherry) signal. White arrowheads mark parallel bundles of actin filaments of filopodia (spike-like protrusions). White arrows indicate F-actin branching in lamellipodia (sheet-like protrusions). Yellow arrowheads show less-adhesive blebbing cells. (D) NC explants of embryos that were injected with 500 pg Trio-GFP in combination with *GAP43-mCherry* RNA. Trio is seen at cell-cell contacts (white arrowheads) or in cell protrusions at the migration front (white arrows). Scale bars: 20 µm.

et al., 1998; Blangy et al., 2000; Debant et al., 1996). Given that RhoA as well as Rac1 can rescue the Trio morphant phenotype, one would expect the GEF1 as well as the GEF2 domain to be essential for migration and cell protrusion formation. To determine this, we co-injected the Trio GEF1 or GEF2 domain together with Trio MO, respectively. *In situ* hybridization for AP-2α revealed that co-injection of GEF2, but not GEF1, significantly restored *in vivo* NC migration (Fig. 4A,B). Moreover, co-injection of GEF2 restored lamellipodia and filopodia formation of Trio morphant NC cells, whereas co-expression of the GEF1 domain resulted in blebbing cells, reminiscent of the morphant NC cells (Fig. 4C). Taken

together, these results indicate that the GEF2, but not the GEF1, domain of Trio is essential for filopodia and lamellipodia formation, and for cranial NC cell migration.

DVL restores migration and protrusion formation of Trio morphant NC cells

In search of molecules that may relay Trio signaling in NC migration, we explored the role of DVL. DVL is a downstream effector of non-canonical Wnt PCP signaling, which has previously been shown to control NC cell migration by affecting RhoA and Rac1 activity (Carmona-Fontaine et al., 2008; De Calisto et al.,
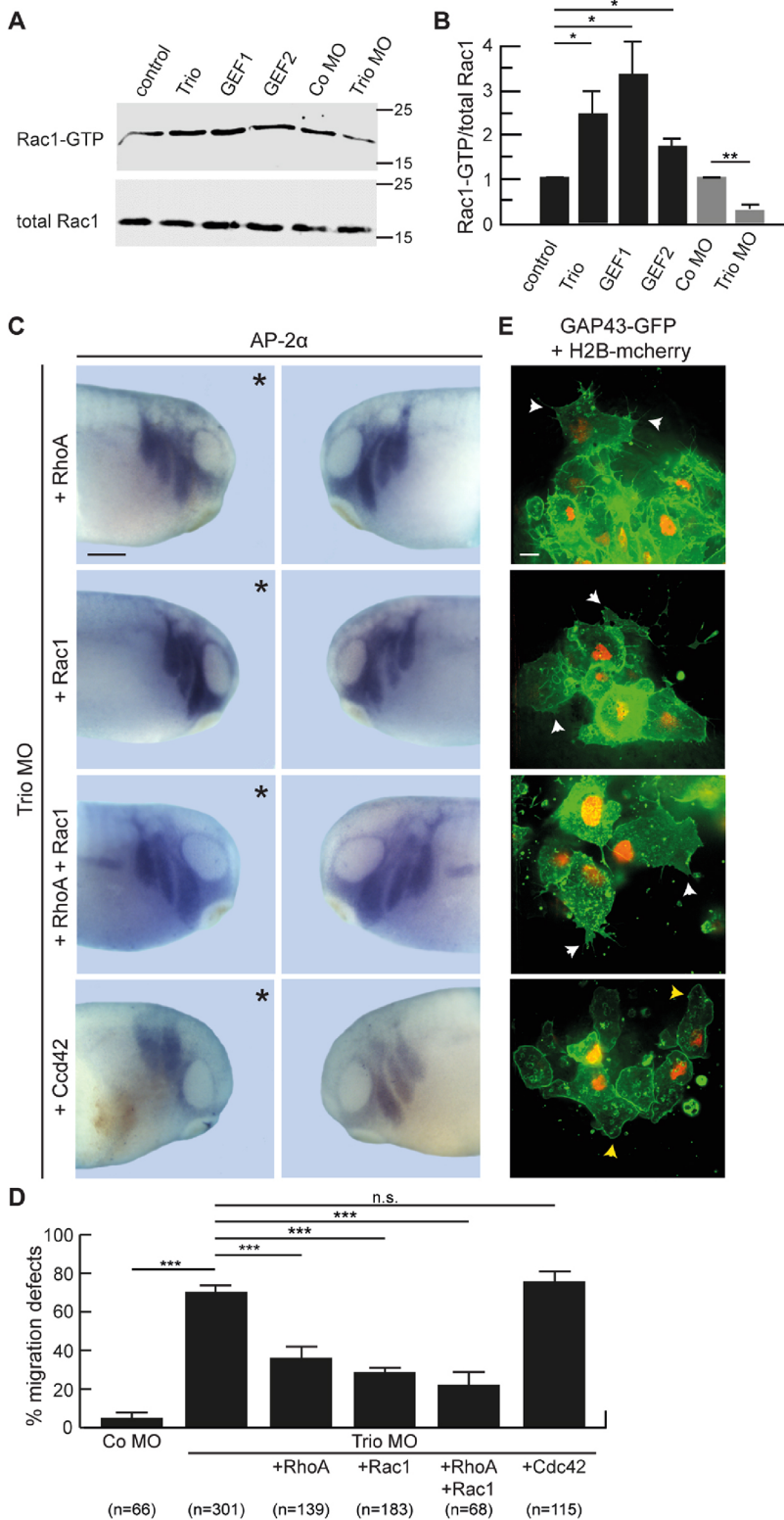
Fig. 3. Activation of RhoA and Rac1, but not Cdc42, rescues the Trio morphant NC defects. (A) Embryos were injected with 100 pg Trio DNA, 250 pg *GEF1* RNA, 250 pg *GEF2* RNA, 5 ng Co MO or 5 ng Trio MO at the one-cell stage. Rac pull-down assays were performed with embryos at stage 20-22. Western blot analysis of Rac1-GTP (upper panel) and total Rac1 (lower panel) are shown. Molecular weights (kDa) are shown on the right. (B) Quantification of Rac1-GTP/total Rac1 from three independent experiments. Data are mean±s.e.m. (C,D) Embryos were injected at the eight-cell stage with 8 ng Trio MO in combination with constitutively active forms of RhoA, Rac1 or Cdc42 (10 pg RhoA, 10 pg Rac1, 5 pg RhoA/5 pg Rac1 or 10 pg Cdc42 DNA). (C) Embryos were analyzed at stage 26 by AP-2α *in situ* hybridization. Asterisk marks the injected side. Scale bar: 250 µm. (D) Graph summarizing the percentage of embryos with NC cell migration defects. Number of embryos (*n*) are indicated for each column. Data are mean±s.e.m. (E) Explants of NC cells injected as in C in combination with 500 pg *GAP43-GFP* and 400 pg *H2B-mcherry* RNA. Yellow arrowheads mark cell blebs; white arrowheads indicate cell protrusions. Scale bar: 20 µm. ***P<0.001, **P<0.01, *P<0.05; n.s., not significant (one-way ANOVA).

2005). Therefore, we analyzed whether DVL is able to rescue the Trio morphant phenotype (Fig. 5). DVL harbors three major conserved domains, the DIX, PDZ and DEP domain, which have been implicated in different downstream signaling events (Boutros and Mlodzik, 1999; Wallingford and Habas, 2005). The DIX domain is used for canonical Wnt signaling, whereas the PDZ domain interacts with canonical and non-canonical Wnt effectors

(Boutros et al., 1998; Habas et al., 2003; Itoh et al., 2000; Rothbächer et al., 2000). The DEP domain has been shown to activate PCP signaling, but recent data also indicate functions in canonical Wnt signaling (Gammons et al., 2016; Paclikova et al., 2017). To analyze whether different DVL activities are able to substitute for Trio function, embryos were injected with Trio MO in combination with either wild-type xDvl2 or the respective deletion

constructs. Indeed, wild-type xDvl2, as well as a xDvl2 construct lacking the DIX domain (ΔDIX), were able to rescue Trio loss-of-function NC cell migration defects (Fig. 5A,B). In contrast, xDvl2 constructs lacking the PDZ (ΔPDZ) or DEP (ΔDEP) domain failed to rescue the Trio morphant phenotype. Overexpression of the different Dvl2 constructs alone did not affect NC migration (Fig. S2). Similar results were obtained analyzing explanted NC cells. Protrusion formation of Trio morphant NC cells was restored by co-expression of xDvl2 or the ΔDIX mutant, while cells co-expressing ΔPDZ or ΔDEP mutants retained a blebbing phenotype (Fig. 5C). Furthermore, as we had shown that Trio activates Rac1 (Fig. 3A), we analyzed whether DVL rescues the Trio morphant phenotype by activating Rac1. Indeed, DVL expression significantly rescues Rac1 activity in Trio morphants (Fig. 5D,E). Thus, these data suggest that DVL acts downstream of Trio – likely by activating Rac1 signaling.

DVL is also able to rescue Cad11 loss-of-function NC migration defects

Previously, we have shown that Trio interacts with Cad11, a calcium-dependent cell-adhesion molecule required for migration and protrusive activity of cranial NC cells (Kashef et al., 2009). Furthermore, Trio expression was able to rescue the Cad11 morphant phenotype (Kashef et al., 2009). Thus, we analyzed whether DVL is also able to rescue the Cad11 loss-of-function phenotype. As previously published (Kashef et al., 2009), Cad11 loss of function inhibited NC cell migration in whole embryos and caused blebbing of explanted NC cells (Fig. 6A-C). Co-expression of xDvl2 significantly rescued the migration defects of Cad11 morphant cells (Fig. 6A,B). Injection of the ΔDIX construct improved the migration defects of Cad11 morphants, but this effect was not significant. In contrast, co-expression of the ΔPDZ or ΔDEP mutants did not rescue the Cad11 morphant phenotype (Fig. 6A-C). Similar effects were observed if cranial cartilage formation was analyzed by Alcian Blue staining of tadpole embryos. While Cad11 MO-injected embryos showed severe defects in cartilage formation on the injected side, these defects were rescued by co-injection of xDvl2 or its ΔDIX mutant (Fig. 6D). In contrast, co-injection of the ΔPDZ or ΔDEP mutants did not restore cranial cartilage formation in Cad11 morphants. Thus, these data indicate that signaling via the DEP and PDZ domains of DVL is able to rescue Cad11 loss of function.

Cad11 does not affect membrane localization of DVL

Activation of Wnt PCP signaling is accompanied by membrane recruitment of DVL, and *Xenopus* ectodermal explants have previously been used to demonstrate Fz-mediated membrane recruitment of DVL (Axelrod et al., 1998; Medina et al., 2000; Medina and Steinbeisser, 2000; Rothbächer et al., 2000; Sheldahl et al., 2003). Therefore, we used this system to analyze whether Cad11 interacts with DVL and recruits this protein to the plasma membrane. Ectodermal explants were injected with myc-tagged *xDvl2* and *GAP43-mCherry* RNA to label the plasma membrane (Fig. 7A). xDvl2 localization was detected in the cytoplasm using confocal microscopy. Co-expression of Fz7-mCherry efficiently recruited xDvl2 to the plasma membrane and intracellular xDvl2 was significantly reduced compared with ectodermal explants expressing only xDvl2 (Fig. 7A,B). In contrast, Cad11-mCherry failed to translocate xDvl2 to the plasma membrane (Fig. 7A,B).

As DVL recruitment to the membrane correlates with its hyperphosphorylation (Rothbächer et al., 2000), we used this readout to further verify our findings. Lysates of ectodermal
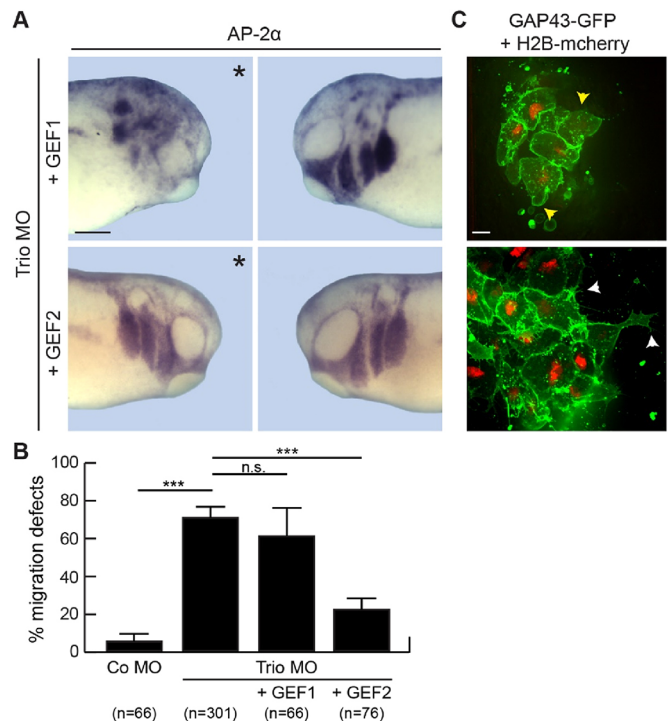

Fig. 4. The GEF2 domain, but not the GEF1 domain, rescues protrusion formation and migration of Trio morphant NC cells. Embryos were injected at the 8-cell stage with 8 ng Trio MO in combination with 10 pg GEF1 or 10 pg GEF2 DNA. (A) Injected embryos were analyzed by AP-2α *in situ* hybridization at stage 26. Asterisks mark the injected side. Scale bar: 250 μm. (B) Graph summarizing the percentage of embryos with NC migration defects. Number of embryos (*n*) is indicated for each column. Data are mean±s.e.m. ***P<0.001; n.s., not significant (one-way ANOVA). (C) Explanted NC cell injected as in A, with the alteration that 500 pg *GAP43-GFP* and 400 pg *H2B-mcherry* RNA were co-injected to mark the membrane (green) and nucleus (red), respectively. Yellow arrowheads mark cell blebs; white arrowheads indicate cell protrusions. Scale bar: 20 μm.

explants expressing myc-tagged xDvl2 alone or in combination with Cad11 were analyzed by western blotting. Explants expressing xDvl2 alone or together with Cad11 showed a xDvl2 band representing non- or poorly phosphorylated xDvl2 (Fig. 7C). However, a prominent high molecular weight band, representing hyperphosphorylated xDvl2, was detected if Fz7 was co-expressed (Fig. 7C). Hyperphosphorylated xDvl2 was also detected in lysates injected with *Fz7* RNA in combination with Cad11 MO or control MO. Thus, Cad11 gain or loss of function does not seem to affect DVL hyperphosphorylation. These data suggest that, although DVL rescues the Cad11 phenotype, these proteins likely do not directly interact. To analyze whether the Cad11 protein physically interacts with DVL, co-immunoprecipitation experiments were performed. Myc-tagged Dvl2 was co-expressed with GFP-tagged Cad11 or β-catenin, and Cad11 was precipitated using anti-GFP antibodies. Although β-catenin co-precipitated with Cad11, Dvl2 did not, further confirming the theory that Cad11 does not directly interact with DVL (Fig. 7D).

DVL interacts with Trio via the C-terminal domain

As DVL does not seem to intersect with the Cad11/Trio signaling cascade at the level of Cad11, we analyzed whether DVL interacts with Trio. Indeed, co-immunoprecipitation experiments showed that HA-tagged Trio was able to co-precipitate Flag-tagged DVL2 in HEK293 lysates (Fig. 8A). In order to map the interaction
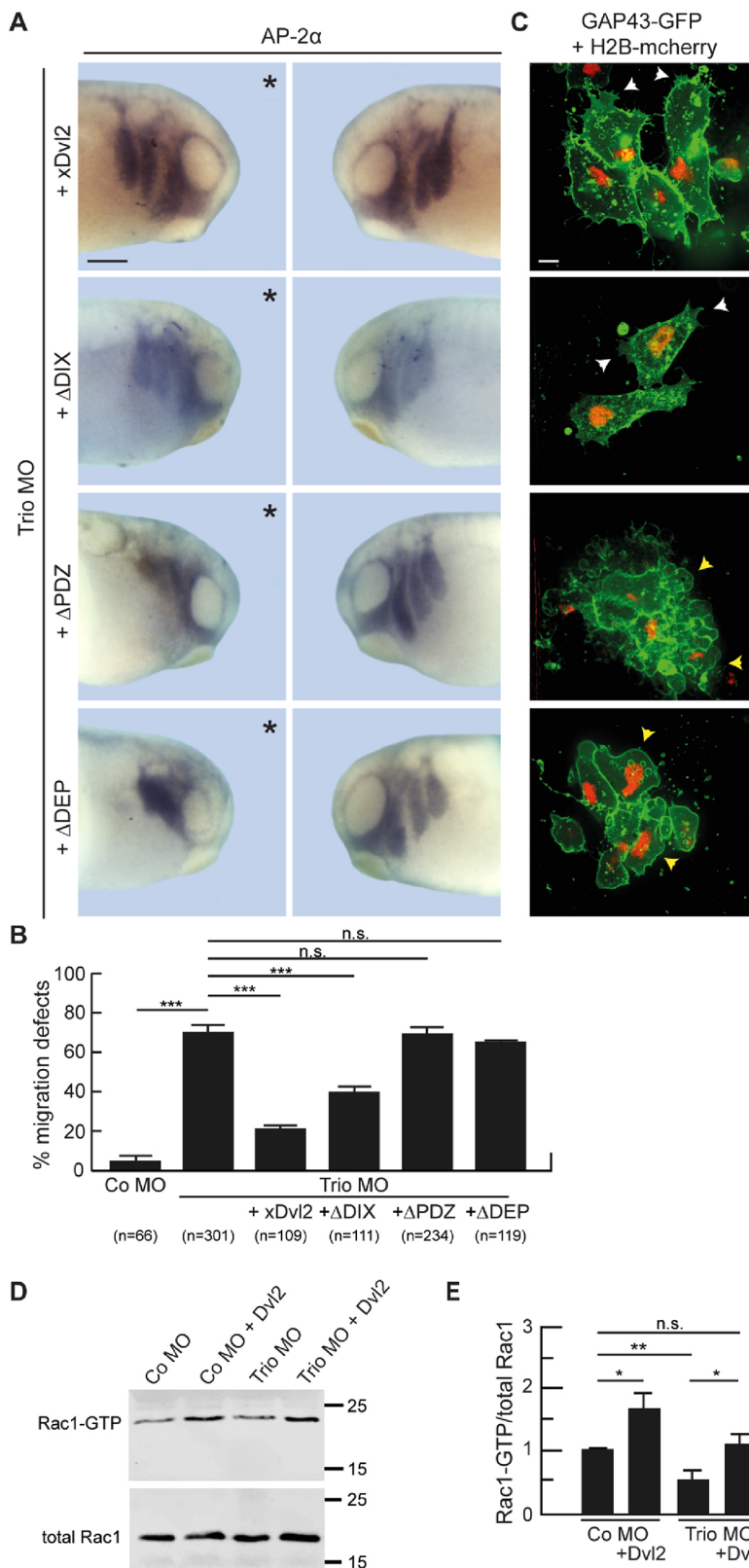
Fig. 5. DVL functionally interacts with Trio and restores protrusion formation and migration in Trio morphant NC cells. (A) Embryos were injected at the 8-cell stage with 8 ng Trio MO in combination with 100 pg *xDvl2*, *ΔDIX*, *ΔPDZ* or *ΔDEP* RNA. NC migration was analyzed by AP-2α *in situ* hybridization. Asterisk marks the injected side. Scale bar: 250 μm. (B) Graph summarizing the percentage of embryos with NC migration defects. Number of embryos (*n*) is indicated for each column. Data are mean±s.e.m. ***P<0.005; n.s., not significant (one-way ANOVA). (C) Explanted NC cell injected as in A, with the addition of 500 pg *GAP43-GFP* and 400 pg *H2B-mcherry* RNA. Yellow arrowheads mark cell blebs; white arrowheads indicate cell protrusions. Scale bar: 20 μm. (D,E) Rac1 activity assay: embryos were injected with 5 ng MO in combination with 300 pg *xDvl2-myc* RNA at the one-cell stage and analyzed at stage 20/21. (D) Western blot analysis of Rac1-GTP (upper panel) and total Rac1 (lower panel) are shown. Molecular weights (kDa) are shown on the right. (E) Quantification of Rac1-GTP/total Rac1 from six (co MO, Trio MO) or three (co MO+Dvl, Trio MO+Dvl) independent experiments. Data are mean±s.e.m. ***P<0.001, **P<0.01, *P<0.05; n.s., not significant (one-way ANOVA).

domain in Trio, we performed further immunoprecipitation experiments expressing its GEF1 or GEF2 constructs (Fig. 8B). Intriguingly, both (i.e. GEF1 or GEF2) domains of Trio revealed some degree of interaction; however, the GEF2 domain appeared to be more effective in precipitating Dvl2 in comparison with GEF1 (Fig. 8B). To further characterize the interaction of DVL with Trio and its truncated variants, we performed immunofluorescence analysis in human HEK293 cells. Full-length DVL is well known to localize into cellular puncta and has a capacity to recruit interacting proteins into these puncta (Schwarz-
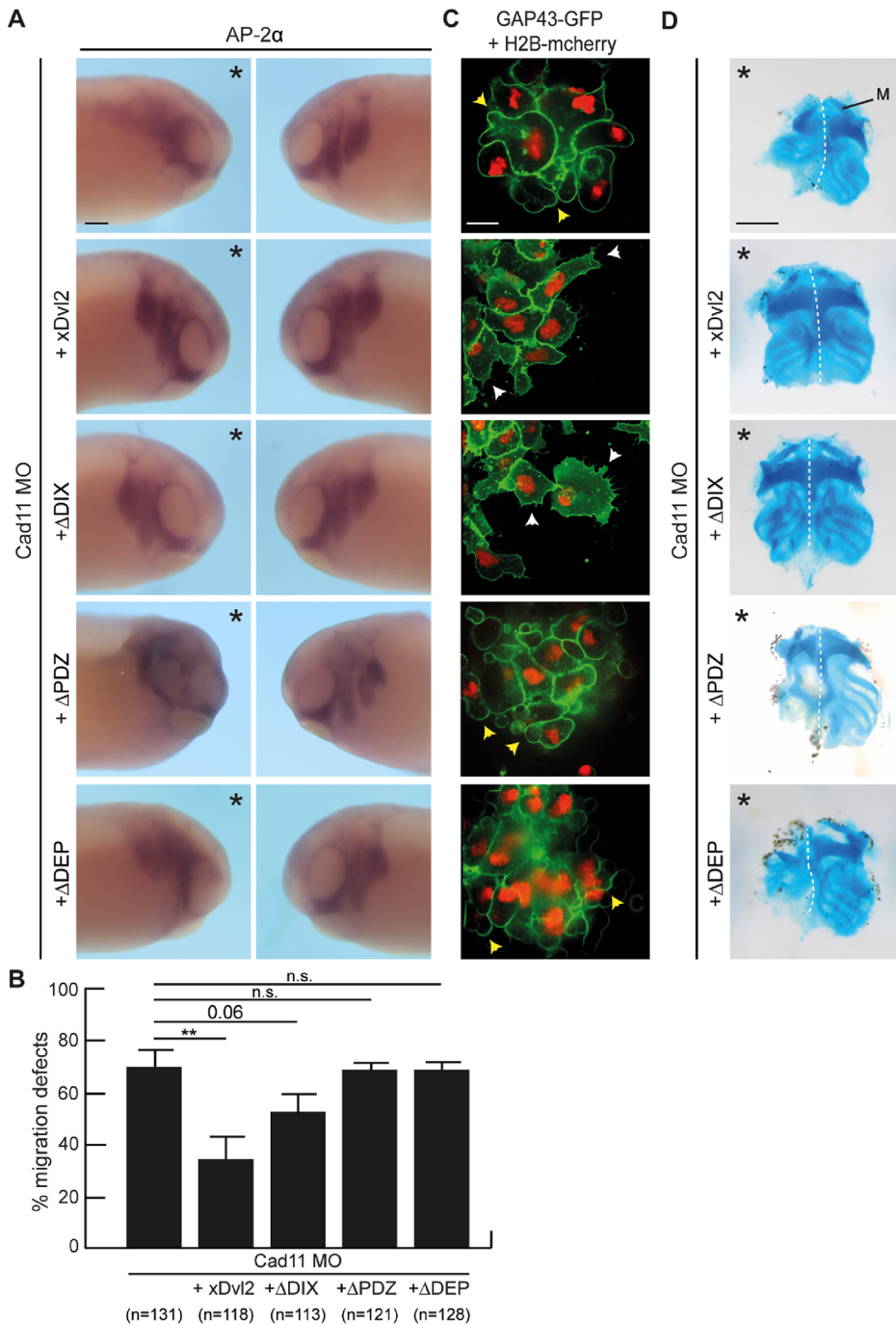
Fig. 6. DVL and DVLΔDIX rescue Cad11 loss-of-function in NC protrusion formation, migration and cartilage formation.
(A) Embryos were injected at the 8-cell stage with 8 ng Cad11 MO in combination with 150 pg *xDvl2*, *ΔDIX*, *ΔPDZ* or *ΔDEP* RNA. NC cell migration was analyzed at stage 26 by AP-2α *in situ* hybridization. Asterisks mark the injected side. Scale bar: 200 µm. (B) Graph summarizing the percentage of embryos with NC migration defects. Number of embryos (*n*) are indicated for each column. Data are mean±s.e.m. ****P*<0.01; n.s., not significant (one-way ANOVA). (C) Explanted NC cells injected as in A with the addition of 150 pg *GAP43-GFP* and 250 pg *H2B-mcherry* RNA. Yellow arrowheads mark cell blebs; white arrowheads indicate cell protrusions. Scale bar: 20 µm. (D) Alcian Blue staining of dissected cartilage structures of tadpole stage embryos injected as in A. Asterisks indicate the injected side. M: Meckel's cartilage. Dashed line indicates the midline of the cartilage structure. Scale bar: 200 µm.

Romond et al., 2005; Smalley et al., 2005). In absence of DVL, Trio as well as its GEF1 and GEF2 domains show an even cytoplasmic localization in HEK293 cells (Fig. 8C,D). However, co-expression of DVL2 completely recruited full-length Trio as well as the Trio GEF2, but not the Trio GEF1 domain, to DVL2-positive dots (Fig. 8E). This suggests that DVL interacts predominantly with the Trio GEF2 domain. In line with the co-immunoprecipitation experiment in Fig. 8B, some degree of colocalization was also detected between GEF1 and DVL2 (white arrows for even localization and yellow arrows for the slight punctae phenotype in Fig. 8E). Taken together, the GEF2 domain of Trio seems to be sufficient for the interaction with DVL, but the GEF1 domain presumably also plays a non-negligible role.

In order to map the interaction domain in DVL, we employed a set of DVL3 truncation mutants (Fig. 8F) (Angers et al., 2006). Trio can efficiently pull down all N-terminally truncated constructs (Fig. 8G), suggesting that Trio interacts with the DVL DEP domain and C-terminus. To further confirm this point for DVL2, we co-transfected DVL2 DEP/C-terminus construct (amino acids 433-736 in human DVL2) with full-length Trio, the Trio GEF1 or the Trio GEF2 domain (Fig. 8H). Indeed, we found that the DEP/C-terminus is sufficient to bind Trio or Trio GEF2 but, unsurprisingly, not GEF1. In summary, these results propose that DVL can interact with Trio and that this binding is mediated mainly by the Trio GEF2 and DVL DEP/C-terminus. Nevertheless, the supportive role of the GEF1 domain of Trio and other parts of DVL
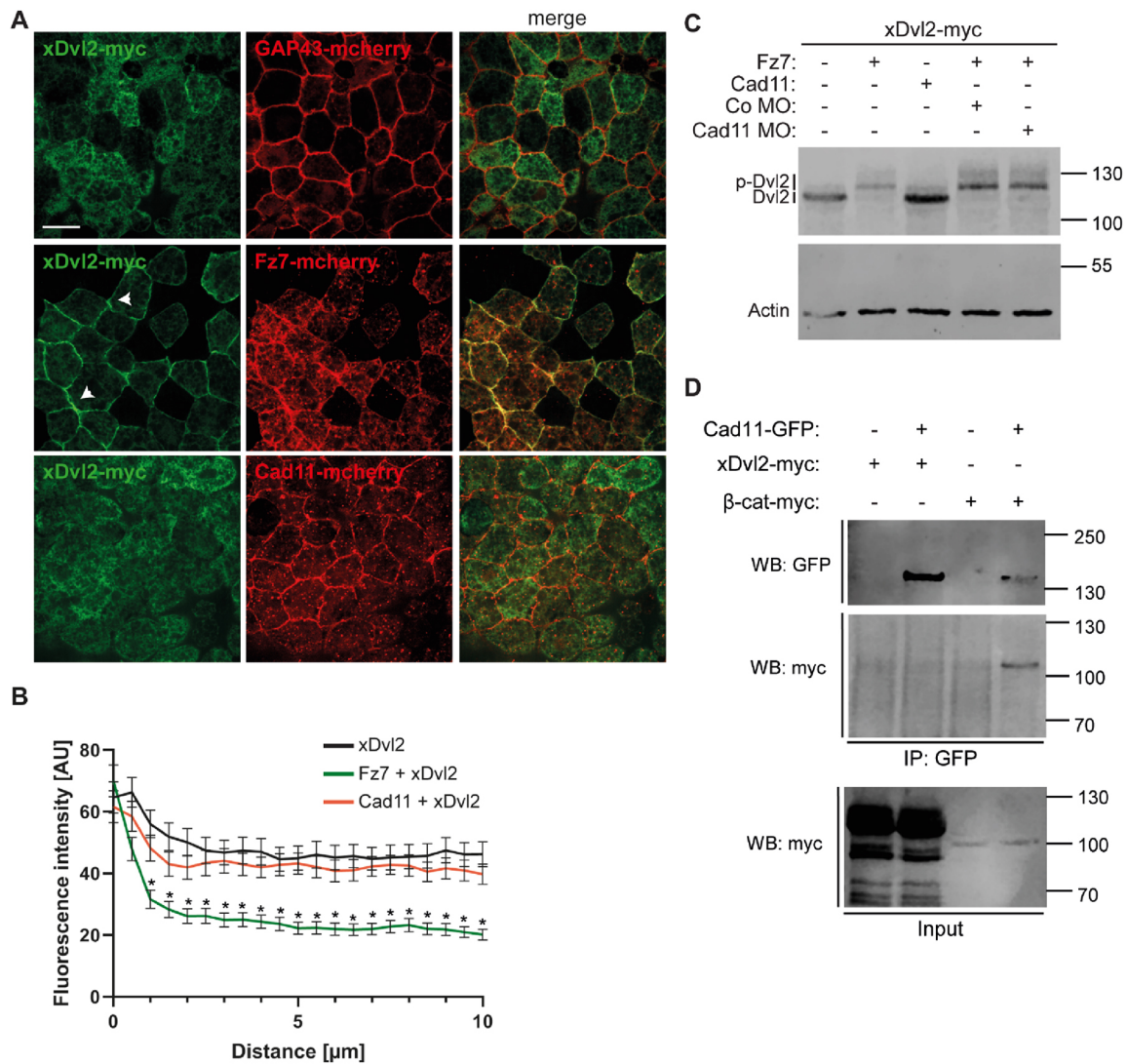
Fig. 7. Trio, but not Cad11, interacts with DVL. (A) DVL localization assay: embryos were injected in both blastomeres at the two-cell stage with 150 pg *xDvl2-myc* and 250 pg *GAP43-mcherry* RNA alone or in combination with 500 pg *Fz7-mcherry* or 500 pg *Cad11-mcherry* RNA. Ectodermal explants were immunostained using anti-Myc antibodies. White arrowheads indicate prominent DVL membrane localization. Scale bar: 20 µm. (B) Graph summarizing the fluorescent intensity across a 10 µm distance from the cell membrane. For each condition, three cells per explant from 19 (Dvl) or 16 (Fz+Dvl, Cad11+Dvl) explants were analyzed (total of 57 or 48 cells). Data are mean±s.e.m. Asterisks indicate significant differences using a non-parametric ANOVA compared with the DVL control. (C) DVL hyperphosphorylation assay: embryos were injected with 100 pg xDvl2, 500 pg *Fz7* or 250 pg *Cad11* RNA and 8 ng MO at the one-cell stage, as indicated, and ectodermal explants were analyzed by western blotting using anti-Myc antibodies. Hyperphosphorylated DVL is detected as high molecular weight band (indicated with pDvl2) compared with non- or poorly phosphorylated Dvl2. (D) Co-immunoprecipitation of DVL or β-catenin with Cad11. Embryos were injected with 500 pg *Cad11-GFP*, 75 pg *xDvl2-myc* or 100 pg *β-catenin-myc* RNA at the one-cell stage. IP, immunoprecipitation; WB, western blotting. Molecular weights (kDa) are shown on the right.

(especially the region between PDZ and DEP) cannot be omitted. Taken together, our data suggest that Trio interacts and signals via DVL to control protrusion formation and migration of cranial NC cells.

DISCUSSION
Migrating NC cells receive multiple signaling inputs, which together need to be relayed to the cytoskeleton to enable directional migration. The Rho GEF Trio is ideally suited to fine-tune signaling, as it contains three different signaling hubs – hence the name Trio – that mediate activation of a number of downstream targets, including different members of the Rho GTPase family. In this study, we have analyzed the function of the Rho GEF Trio in

NC development and demonstrate that it is required for protrusion formation and migration of cranial NC cells, as well as development of the craniofacial cartilage. We propose a model (Fig. 9) whereby Trio enables protrusion formation by interacting with DVL to activate Rac1.

(1) We find that Trio interacts with DVL via the DEP/C-terminal domain of DVL, as well as the GEF2 domain of Trio.

(2) DVL rescued protrusion formation as well as *in vivo* migration of Trio morphant NC cell. This is likely mediated by DVL-mediated activation of Rac1, because DVL restores Rac1 activity in Trio morphant embryos.

(3) Rescue experiments demonstrate that the Trio GEF2 domain, which binds DVL, is sufficient to rescue Trio loss of function.
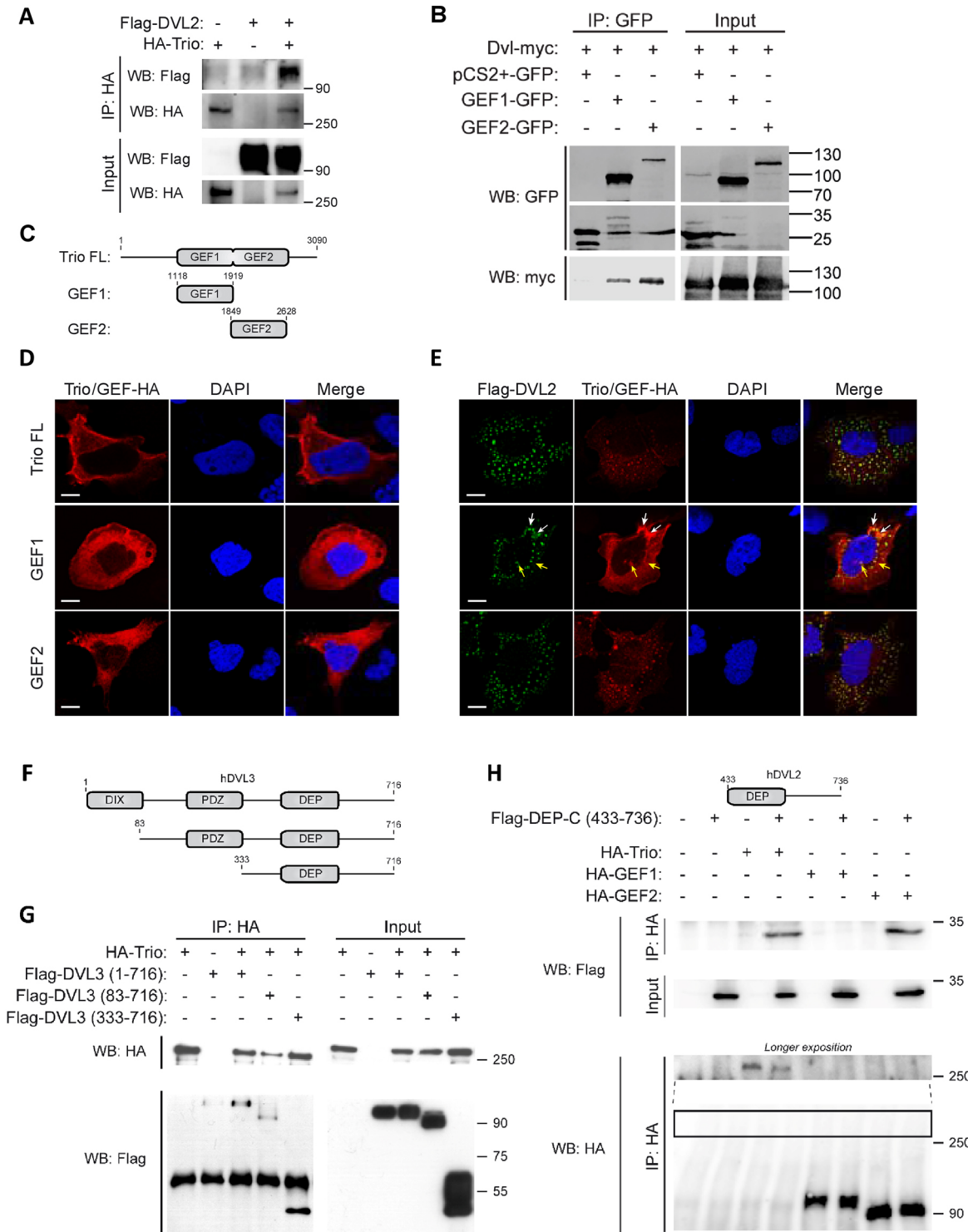
Fig. 8. Interaction of DVL and Trio. (A) Flag-DVL2 and HA-Trio were co-transfected in HEK293 cells and immunoprecipitated as indicated. (B) XDvl2-myc and *Xenopus* GEF1 or GEF2 domains expressed in HEK293 cells were immunoprecipitated with anti-GFP antibody, and DVL2 present in the complex was detected using anti-Myc antibodies. pCS2+-GFP, which contains only GFP, was used as a negative control. (C) Schematics of the human Trio constructs used in D,E,H. (D,E) Subcellular localization of HA-tagged Trio constructs in the absence (D) or presence (E) of Flag-DVL2. Evenly distributed full-length Trio and Trio-GEF2 (D) are efficiently recruited to DVL2 dots (E). Some degree of colocalization was also detected for GEF1 and DVL2 (white arrows indicate even localization, yellow arrows the slight punctae phenotype). (F) Schematics of DVL3 truncation constructs used in G. (G) All DVL3 constructs that contain the DEP/C terminus efficiently co-immunoprecipitated with Trio in HEK293 cells. (H) DEP/C-terminus of DVL2 and GEF2 of Trio are sufficient for interaction of DVL and Trio. IP, immunoprecipitation; WB, western blotting. Molecular weights (kDa) are shown on the right. All experiments shown in this figure were performed in biological triplicates.

The Trio/DVL/Rac1 signaling module likely functions downstream of Cad11, because all these components are able to rescue Cad11 loss of function and a biochemical interaction of Cad11 and Trio has previously been demonstrated (Kashef et al., 2009). Thus, these data reveal a novel signaling function for Trio via DVL in protrusion formation of NC cells.
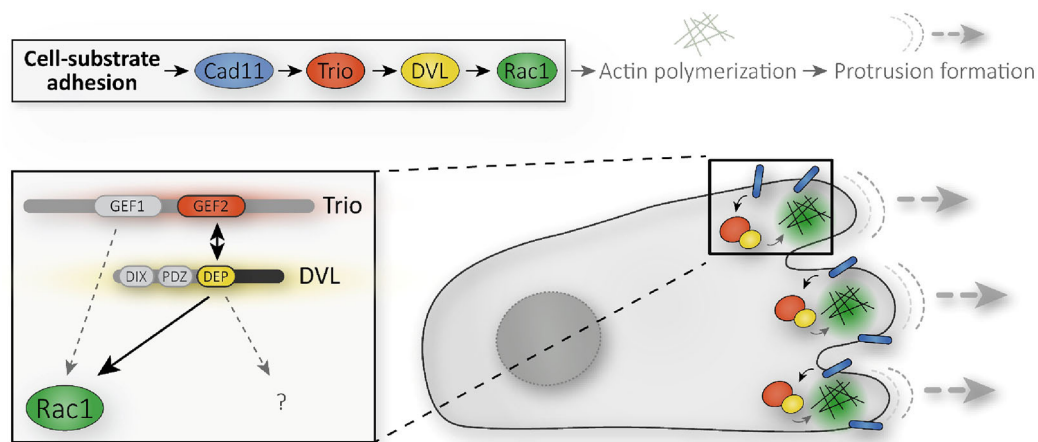
Fig. 9. Trio promotes protrusion formation of NC cells by interacting with Dvl and activating Rac1. The image depicts a migrating NC cell. Trio is shown in red, Dvl in yellow, Cad11 in blue and activated Rac1 in green. The proposed signaling cascade leading to protrusion formation is shown at the top. A higher magnification of the Trio/Dvl interaction leading to activation of Rac1 is shown on the left. Findings presented in this study are highlighted in the black box and by black arrows. See Discussion for further details.

Both Trio and DVL have previously been implicated in the control of NC migration; however, functional interaction of both proteins has not been demonstrated yet. DVL is a key molecule of the Wnt signaling pathway and a known player of Wnt PCP signaling (Gao and Chen, 2010). In *Xenopus*, xDvl1 and xDvl2 are expressed in migratory cranial NC cells (Gray et al., 2009) and different DVL deletion mutants have been used to demonstrate a role for non-canonical Wnt signaling in the regulation of NC migration (De Calisto et al., 2005). Furthermore, membrane recruitment of DVL – indicative of activation of non-canonical Wnt PCP signaling – has been demonstrated in NC cells undergoing contact inhibition of locomotion (Carmona-Fontaine et al., 2008). Like DVL, Trio has also been implicated in the control of NC cell migration. Trio is expressed in *Xenopus* migratory cranial NC cells (Kratzer et al., 2019) and has been shown to interact with Cad11, a known regulator of NC cell migration (Becker et al., 2013; Borchers et al., 2001; Kashef et al., 2009; Langhe et al., 2016). Moreover, Trio interacts with Par3, a polarity protein required for contact inhibition of locomotion (Moore et al., 2013). In the presented study, we provide evidence for a functional and physical interaction of Trio with DVL. First, we note that DVL rescues Trio loss of function, an activity requiring the PDZ and DEP domains of DVL. Second, we show that both proteins interact in human cells via the DEP/C terminus of DVL and the GEF2 domain of Trio. This interaction likely takes place in the cytoplasm, as full-length Trio and its GEF2 domain localized to intracellular DVL-positive punctae – possibly representing signalosomes (Gammons et al., 2016) – in HEK293 cells. Furthermore, we did not find evidence for the formation of a trimeric complex of Cad11/Trio and DVL, as Cad11 did not interact with DVL or recruit it to the plasma membrane. In addition, we also failed to observe hyperphosphorylation of DVL – either in presence of Cad11 or Trio (Fig. S3). Thus, the Trio/DVL interaction likely does not require Cad11; however, Cad11 likely activates the Trio/Dvl module by interacting with Trio.

The multifunctional Rho GEF Trio may play different roles, depending on subcellular localization. In cell protrusions Trio can be part of a complex with Cad11, which is prominently localized in cell protrusions (Kashef et al., 2009). As we find that Trio activates Rac1 at stages of cranial NC cell migration, this complex likely supports protrusion formation by activating Rac1. Furthermore,

DVL interacts with Trio and rescues protrusion formation and migration of Cad11 and Trio morphants, indicating that Trio signaling via DVL and Rac1 is active in protrusion formation. Moreover, Trio loss-of-function decreases embryonic Rac1 activity and this can be rescued by DVL expression. Indeed, DVL has been shown to interact and activate Rac1 (Cajanek et al., 2013; Habas et al., 2003), e.g. by interacting with the Rac1 GEF Tiam (Cajanek et al., 2013). Thus, DVL may activate Rac1 by acting as a scaffold to bring Rho GEFs, such as Trio, in close proximity to Rac1. This may also explain why Trio alone cannot rescue the decrease in Rac1 activity of DVL morphants (Fig. S4). Surprisingly, although the GEF1 domain activates Rac1, it is not sufficient to rescue the Trio morphant phenotype. In contrast, the GEF2 domain, which binds DVL, is able to rescue Trio loss of function. This suggests that – in addition to activation of Rac1 signaling – interaction with DVL may have additional qualities that are required to stimulate NC migration. For example, NC migration is probably not exclusively mediated by Rac1 activation, but may also involve activation of RhoA, because constitutive active Rac1 as well as RhoA rescue protrusion formation and migration of Trio morphant NC cells. Whether Rac1 and RhoA activation are two independent events or are caused by the ability of small GTPases of the Rho family to bidirectionally affect their activity (Burridge and Wennerberg, 2004) is currently unclear. However, we observed that embryonic RhoA activity is relatively low at stages of cranial NC migration. Thus, loss of function of Trio does not lead to a prominent decrease, although ectopic expression of Trio or its GEF2 domain activates RhoA signaling (Fig. S5). Taken together, these data suggest that Trio promotes NC protrusion formation by interacting with DVL. This leads to activation of Rac1, but may also affect other yet unknown signaling mechanisms.

Although our data suggest Trio activity is required in nascent NC cell protrusions, the situation may be different at NC cell-cell contact zones. Moore et al. showed that Par3 is required for contact inhibition of locomotion and promotes microtubule catastrophe by inhibiting Trio Rac1-GEF activity at cell-cell contacts (Moore et al., 2013). Thus, at the cell-cell-contact zone, Par3 interacts with Trio, thereby preventing it from activating Rac1. As Rac1 promotes microtubule stability, inhibition of Trio results in microtubule catastrophe at cell-cell contact sites, a reversal of cell polarity and a

change in the direction of migration. Although Moore et al. suggest that Par3 inhibits Trio GEF activity, a recent report proposes that Par3 also exerts positive effects on Trio (Landin Malt et al., 2019). In the inner ear, Par3 is essential for planar cell polarity of hair cells and interacts with Trio to activate a Rac1-Pak signaling pathway. In this scenario, Par3 regulates the activity of microtubule-associated proteins and contributes to the stability of microtubules. Whether Par3/Trio signaling intersects with Cad11/Trio signaling and whether DVL plays a role in such a signaling event is currently unknown. Taken together, these data suggest that Trio has different functions in NC cell migration depending on the subcellular localization. Future research will have to dissect the underlying distinct signaling activities, as well as the molecular mechanisms that accomplish their control. As Trio, Cad11 and DVL are expressed in a variety of different cell types, our results may uncover a general function of these molecules in mediating cell migration, and may contribute to a better understanding of cell migration and cell invasion in a variety of diseases.

MATERIALS AND METHODS
Constructs
Trio and Cad11 morpholino antisense oligonucleotides were used as published previously (Kashef et al., 2009). An additional Trio MO, Trio MO2 (5′-ATCCTTAGAGTTCCCCAACCCTCCA-3′), targeted to the 5′-UTR region was generated by Gene Tools. As a control, a standard control MO from Gene Tools was used. The following plasmids were used for RNA or DNA *Xenopus* injection: Cad11 (Borchers et al., 2001), Cad11-myc (Langhe et al., 2016), Cad11-GFP (Kashef et al., 2009), Fz7 (Medina et al., 2000), Fz7-myc (Winklbauer et al., 2001), GAP43-mCherry and GAP43-GFP (Moriyoshi et al., 1996), H2B-mCherry (Kashef et al., 2009), Lifeact-mCherry (Riedl et al., 2008), constitutively active RhoA, Rac1 and Cdc42 (Schambony and Wedlich, 2007), Trio-HA (Kashef et al., 2009), Trio-GEF1-HA and Trio-GEF2-HA (Debant et al., 1996), Trio-GFP (Moore et al., 2013), xDvl2-GFP (Yang-Snyder et al., 1996), xDvl2-myc (Sokol, 1996), and xDvl2ΔDIX, xDvl2ΔPDZ and xDvl2ΔDEP (Miller et al., 1999) cloned in pCS2+. For transfection of human cells, DVL3 wt-Flag and truncated variants (Angers et al., 2006) and DVL2-Flag (Narimatsu et al., 2009) were used.

For cloning of the *Xenopus* GEF constructs, the coding sequence, containing the DH, PH and SH3 domain of Trio-GEF1 (3784-5197 bp) or GEF2 (5791-8016 bp), was amplified by PCR from cDNA of *Xenopus laevis* embryos. C-terminal eGFP-tagged *Xenopus* GEF constructs were generated using the following primers with ClaI/XhoI restriction sites: GEF1-forward, 5′-ATCGATATGGGTTCCGAAGTGAAGCTTCG-3′; GEF1-reverse, 5′-C-TCGAGGACAGAGAGGGAATCTTTGTGGT-3′; GEF2-forward, 5′-AT-CGATATGGGTGACAGTAGTAGCCCATCG-3′; GEF2-reverse, 5′-CTC-GAGAAACTCTGGGGGAGCATCATA-3′. The PCR product was cut with ClaI and XhoI, and cloned into the respective sites of pCS2+/eGFP.

Embryo manipulation, whole-mount *in situ* hybridization, cartilage staining and imaging
Xenopus laevis embryos were obtained by *in vitro* fertilization and staged according to Nieuwkoop and Faber (Nieuwkoop and Faber, 1967). All procedures were performed according to the German animal use and care law (Tierschutzgesetz) and approved by the German state administration Hesse (Regierungspräsidium Giessen). RNA was synthesized *in vitro* using the mMessage mMachine Kit (Ambion). If not indicated otherwise, injections were performed into one of the animal dorsal blastomeres of 8-cell stage embryos to target the NC. Fluorescein-dextran (4 ng 10,000 MW, ThermoFisher Scientific), *GAP43-GFP* RNA (500 pg), *GAP43-mcherry* RNA (500 pg) or *H2B-mcherry* RNA (400 pg) were used as lineage tracer, membrane or nuclear marker, respectively. For whole-mount *in situ* hybridization (Harland, 1991), digoxigenin-labeled antisense RNA probes were generated according to the manufacturer's instructions (Roche) using AP-2α (Luo et al., 2003). NC cell migration was rated as defective when the hyoid and branchial branches did not migrate at least half of the distance

compared with the control side. Analysis were performed double-blind, whereby the person scoring the neural crest defects was not aware of the respective treatments of the embryos. Significances were tested with one-way ANOVA followed by Tukey's or Dunnett's post-hoc multiple comparison test using Prism8 (GraphPad). NC transplantations, NC explants and cartilage staining were performed as previously described (Kashef et al., 2009).

Ectodermal explants (animal caps) were dissected at stage 8/9 and fixed at stage 11 in 4% paraformaldehyde. Immunostaining was carried out as previously described (Yang-Snyder et al., 1996) with anti-Myc antibodies (9E10, M5546 Sigma, 1:2000) and anti-mouse Alexa Fluor 594 (A-11005 ThermoFisher Scientific, 1:400). Dvl fluorescence intensity was quantified using ImageJ. To this end, a straight line was drawn from the cell membrane (indicated by the mCherry or RFP signal in the red channel) to the cytoplasm, the cell nucleus was avoided. The line was transferred to the green channel of the Dvl-myc signal and the fluorescence intensity was measured. A line was drawn of three random cells per explant. Statistical analysis was performed with Prism using a two-way ANOVA. For western blot analysis, 20 animal caps were homogenized at stage 11 in 200 μl lysis buffer [50 mM Tris (pH 7.5), 150 mM NaCl, 0.5% Nonidet P40] containing protease and phosphatase inhibitor cocktail tablets (Roche). Myc-tagged DVL protein was detected by western blot using primary anti-Myc (9E10, M5546 Sigma, 1:2000) and anti-actin (MAB1501, Sigma, 1:1000) and secondary anti-mouse-IRDye 680CW (LI-COR, 926-32212, 1:7500). The infrared signals were detected by LI-COR Odyssey Fc System and analyzed by Image Studio Software (LI-COR).

Trio expression in whole embryos was analyzed by western blotting using lysates of stage 12 embryos. Trio protein was detected using anti-Trio antibodies (HPA064664, Sigma, 1:50). As a loading control, actin was detected using an anti-actin (MAB1501, Sigma, 1:1000).

Embryos were imaged using a Leica MZ16F stereo-microscope. NC and ectodermal explants were analyzed using spinning disc confocal microscopy [Axio Observer Z1 with 63× or 40× plan apochromat NA 1.4 oil objective using AxioVision 4.8.2 or ZEN software (Zeiss)] or fluorescence microscope [Axio Observer Z1 with Apotome and 63× plan apochromat NA 1.4 oil objective using AxioVision 4.8 (Zeiss)]. Cell circularity of NC cells was measured by ImageJ using the formula $4\pi(area/perimeter^2)$. Statistical analysis was performed using Prism8 (GraphPad). Normality of datasets was tested using D'Agostine and Pearson test, Shapiro-Wilk test and Kolmogorov–Smirnov test. Datasets that did not show normal distribution were compared using non-parametric ANOVA with Kruskal–Wallis multiple comparison test.

Co-immunoprecipitation
HEK293 cells were cultivated on 25 cm² cell culture flasks and transfected with DNA plasmids using JetPEI (Polyplus Transfection) according to the manufacturer's instructions. 48 h after transfection, the cells were washed twice with ice-cold 1× PBS, scraped and lysed in NOP-lysis buffer [150 mM NaCl, 10 mM HEPES (pH 7.4), 2 mM EDTA, 1% Nonidet P40 and 0.1% SDS] containing protease and phosphatase inhibitor cocktail tablets (Roche). Co-immunoprecipitation with Protein A-Sepharose CL-4B (GE Healthcare) (Cad11-Dvl2 Co-IP) was carried out as previously reported (Berger et al., 2017) using anti-GFP (Abcam, ab290, 1 μg) for antigen-antibody reaction. Co-immunoprecipitations with Pierce Co-Immunoprecipitation Kit (GEF-DVL Co-IPs) were performed according to the manufacturer's instructions using anti-GFP (Abcam, ab290, 1:200) antibodies. Antibody-resin coupling was carried out for 1 h and antigen-antibody reaction for 1 h at 4°C. Proteins were detected by western blot using different antibodies: anti-GFP (Abcam, ab290, 1:2000), anti-Myc (9E10, M5546 Sigma, 1:2000), anti-Flag (Sigma, F7425, 1:1000) and anti-HA.11 (MMS-101R, Covance, 1:1000) as primary antibodies and anti-rabbit-IRDye 800CW (926-32213, LI-COR, 1:7500), anti-mouse-IRDye 680RD (926-68072, LI-COR, 1:7500) and anti-rabbit IgG (whole molecule) peroxidase antibody (Sigma, A0545 1:5000) as secondary antibodies. Western blot samples were developed digitally using the chemiluminescence documentation system FusionSL (Vilber-Lourmat) or Infrared signals were detected by LI-COR Odyssey Fc System and analyzed by Image Studio Software (LI-COR).

Embryos were injected at the one-cell stage with 500 pg *Cad11-GFP*, 75 pg *xDvl2-myc* and 100 pg *β-catenin-myc* RNA (Fagotto et al., 1996), and cultured until stage 11. For co-immunoprecipitation, 50 embryos of each condition were lysed in 500 µl NOP-lysis buffer containing protease inhibitor (Roche). Co-immunoprecipitation was performed with Dynabeads Protein G Immunoprecipitation Kit according to the manufacturer's protocol using anti-GFP antibodies (Abcam, ab290, 1:250). Proteins were detected by western blot using the following antibodies: anti-GFP (Roche, 11814460001, 1:1000) and anti-Myc (Abcam, ab19234, 1:1000), anti-mouse-IRDye 680CW (LI-COR, 926-32212, 1:7500) and anti-goat-IRDye 800CW (LI-COR, 926-32214, 1:7500). Infrared signals were detected by LI-COR Odyssey Fc System and analyzed by Image Studio Software (LI-COR).

Immunofluorescence of human cells
HEK293 cells (HEK293T ATCC-CRL-11268, tested regularly for mycoplasma contamination) were seeded on gelatin-coated coverslips in 24-well plates and were transfected the next day with 100 ng of each plasmid. 24 h later, cells were fixed in fresh 4% paraformaldehyde, permeabilized with 0.5% Triton X-100, blocked with PBS/BSA/Triton/Azide buffer (PBTA) [3% (w/v) BSA, 0.25% Triton, 0.01% NaN$_3$] for 1 h, and incubated overnight with primary antibodies in PBTA at 4°C. The next day, the coverslips were washed in 3× PBS and incubated for 2 h with secondary antibodies conjugated to Alexa Fluor 488 (Invitrogen, A11001, 1:1000) and Alexa Fluor 594 (Invitrogen, A11058, 1:1000). Subsequently, the samples were washed 4× with PBS and 1× DAPI (1:5000 in PBS), and the coverslips were mounted on microscopic slides. The samples were then visualized on an Olympus Fluoview 500 confocal laser scanning microscope IX71 using a 100× oil objective. The primary antibodies used were as follows: anti-FLAG M2 (Sigma, F1804, 1:1000) and anti-HA (Abcam, ab9110, 1:1000).

RhoA/Rac activity assays
Xenopus embryos were co-injected with RNA or MO together with 4 ng fluorescein-dextran to distinguish injected from uninjected embryos. Control embryos were injected only with fluorescein-dextran. Twenty-five stage 20-22 embryos were collected for each condition and lysed in 250 µl Rac-RIPA buffer [50 mM Tris (pH 7.2), 150 mM NaCl, 10 mM MgCl$_2$, 1% Triton X-100, 0.1% SDS, complete protease inhibitor mix (Roche)]. As a positive control, lysates of 25 wild-type embryos of stage 20/21 were incubated with GTPγS (Sigma-Aldrich) according to the manufacturer's instructions. Rho or Rac pull-down assays were performed as described previously (Benard et al., 1999; Ren et al., 1999). Samples were loaded on 12% SDS PAGE gels and detection of proteins was carried out using anti-Rac1 (1:1000, mouse, BD Biosciences 610651), anti-RhoA (1:500, mouse, Santa Cruz sc-418) and anti-mouse-IRDye 800 (1:7500, Li-COR 926-68072) antibodies. Significances were tested with one-way ANOVA.

References
Abercrombie, M. and Heaysman, J. E. M. (1953). Observations on the social behaviour of cells in tissue culture. I. Speed of movement of chick heart fibroblasts in relation to their mutual contacts. *Exp. Cell Res.* **5**, 111-131. doi:10.1016/0014-4827(53)90098-6

Angers, S., Thorpe, C. J., Biechele, T. L., Goldenberg, S. J., Zheng, N., MacCoss, M. J. and Moon, R. T. (2006). The KLHL12-Cullin-3 ubiquitin ligase negatively regulates the Wnt-β-catenin pathway by targeting Dishevelled for degradation. *Nat. Cell Biol.* **8**, 348-357. doi:10.1038/ncb1381

Axelrod, J. D., Miller, J. R., Shulman, J. M., Moon, R. T. and Perrimon, N. (1998). Differential recruitment of Dishevelled provides signaling specificity in the planar cell polarity and Wingless signaling pathways. *Genes Dev.* **12**, 2610-2622. doi:10.1101/gad.12.16.2610

Ba, W., Yan, Y., Reijnders, M. R. F., Schuurs-Hoeijmakers, J. H. M., Feenstra, I., Bongers, E. M. H. F., Bosch, D. G. M., De Leeuw, N., Pfundt, R., Gilissen, C. et al. (2016). TRIO loss of function is associated with mild intellectual disability and affects dendritic branching and synapse function. *Hum. Mol. Genet.* **25**, 892-902. doi:10.1093/hmg/ddv618

Backer, S., Hidalgo-Sanchez, M., Offner, N., Portales-Casamar, E., Debant, A., Fort, P., Gauthier-Rouviere, C. and Bloch-Gallego, E. (2007). Trio controls the mature organization of neuronal clusters in the hindbrain. *J. Neurosci.* **27**, 10323-10332. doi:10.1523/JNEUROSCI.1102-07.2007

Bajanca, F., Gouignard, N., Colle, C., Parsons, M., Mayor, R. and Theveneau, E. (2019). In vivo topology converts competition for cell-matrix adhesion into directional migration. *Nat. Commun.* **10**, 1518. doi:10.1038/s41467-019-09548-5

Becker, S. F. S., Mayor, R. and Kashef, J. (2013). Cadherin-11 mediates contact inhibition of locomotion during Xenopus neural crest cell migration. *PLoS ONE* **8**, e85717. doi:10.1371/journal.pone.0085717

Bellanger, J.-M., Lazaro, J.-B., Diriong, S., Fernandez, A., Lamb, N. and Debant, A. (1998). The two guanine nucleotide exchange factor domains of Trio link the Rac1 and the RhoA pathways in vivo. *Oncogene* **16**, 147-152. doi:10.1038/sj.onc.1201532

Bellanger, J.-M., Astier, C., Sardet, C., Ohta, Y., Stossel, T. P. and Debant, A. (2000). The Rac1- and RhoG-specific GEF domain of Trio targets filamin to remodel cytoskeletal actin. *Nat. Cell Biol.* **2**, 888-892. doi:10.1038/35046533

Benard, V., Bohl, B. P. and Bokoch, G. M. (1999). Characterization of rac and cdc42 activation in chemoattractant-stimulated human neutrophils using a novel assay for active GTPases. *J. Biol. Chem.* **274**, 13198-13204. doi:10.1074/jbc.274.19.13198

Berger, H., Breuer, M., Peradziryi, H., Podleschny, M., Jacob, R. and Borchers, A. (2017). PTK7 localization and protein stability is affected by canonical Wnt ligands. *J. Cell Sci.* **130**, 1890-1903. doi:10.1242/jcs.198580

Blangy, A., Vignal, E., Schmidt, S., Debant, A., Gauthier-Rouviere, C. and Fort, P. (2000). TrioGEF1 controls Rac- and Cdc42-dependent cell structures through the direct activation of rhoG. *J. Cell Sci.* **113**, 729-739.

Borchers, A., David, R. and Wedlich, D. (2001). Xenopus cadherin-11 restrains cranial neural crest migration and influences neural crest specification. *Development* **128**, 3049-3060.

Boutros, M. and Mlodzik, M. (1999). Dishevelled: at the crossroads of divergent intracellular signaling pathways. *Mech. Dev.* **83**, 27-37. doi:10.1016/S0925-4773(99)00046-5

Boutros, M., Paricio, N., Strutt, D. I. and Mlodzik, M. (1998). Dishevelled activates JNK and discriminates between JNK pathways in planar polarity and wingless signaling. *Cell* **94**, 109-118. doi:10.1016/S0092-8674(00)81226-X

Burridge, K. and Wennerberg, K. (2004). Rho and Rac take center stage. *Cell* **116**, 167-179. doi:10.1016/S0092-8674(04)00003-0

Cajanek, L., Ganji, R. S., Henriques-Oliveira, C., Theofilopoulos, S., Konik, P., Bryja, V. and Arenas, E. (2013). Tiam1 regulates the Wnt/Dvl/Rac1 signaling pathway and the differentiation of midbrain dopaminergic neurons. *Mol. Cell. Biol.* **33**, 59-70. doi:10.1128/MCB.00745-12

Carmona-Fontaine, C., Matthews, H. K., Kuriyama, S., Moreno, M., Dunn, G. A., Parsons, M., Stern, C. D. and Mayor, R. (2008). Contact inhibition of locomotion in vivo controls neural crest directional migration. *Nature* **456**, 957-961. doi:10.1038/nature07441

Charrasse, S., Comunale, F., Fortier, M., Portales-Casamar, E., Debant, A. and Gauthier-Rouvière, C. (2007). M-cadherin activates Rac1 GTPase through the Rho-GEF trio during myoblast fusion. *Mol. Biol. Cell* **18**, 1734-1743. doi:10.1091/mbc.e06-08-0766

De Calisto, J., Araya, C., Marchant, L., Riaz, C. F. and Mayor, R. (2005). Essential role of non-canonical Wnt signalling in neural crest migration. *Development* **132**, 2587-2597. doi:10.1242/dev.01857

Debant, A., Serra-Pages, C., Seipel, K., O'Brien, S., Tang, M., Park, S. H. and Streuli, M. (1996). The multidomain protein Trio binds the LAR transmembrane

DEVELOPMENT

13

tyrosine phosphatase, contains a protein kinase domain, and has separate rac-specific and rho-specific guanine nucleotide exchange factor domains. *Proc. Natl. Acad. Sci. USA* **93**, 5466-5471. doi:10.1073/pnas.93.11.5466

Fackler, O. T. and Grosse, R. (2008). Cell motility through plasma membrane blebbing. *J. Cell Biol.* **181**, 879-884. doi:10.1083/jcb.200802081

Fagotto, F., Funayama, N., Gluck, U. and Gumbiner, B. M. (1996). Binding to cadherins antagonizes the signaling activity of beta-catenin during axis formation in Xenopus. *J. Cell Biol.* **132**, 1105-1114. doi:10.1083/jcb.132.6.1105

Gammill, L. S., Gonzalez, C., Gu, C. and Bronner-Fraser, M. (2006). Guidance of trunk neural crest migration requires neuropilin 2/semaphorin 3F signaling. *Development* **133**, 99-106. doi:10.1242/dev.02187

Gammill, L. S., Gonzalez, C. and Bronner-Fraser, M. (2007). Neuropilin 2/semaphorin 3F signaling is essential for cranial neural crest migration and trigeminal ganglion condensation. *Dev. Neurobiol.* **67**, 47-56. doi:10.1002/dneu.20326

Gammons, M. V., Renko, M., Johnson, C. M., Rutherford, T. J. and Bienz, M. (2016). Wnt signalosome assembly by DEP domain swapping of dishevelled. *Mol. Cell* **64**, 92-104. doi:10.1016/j.molcel.2016.08.026

Gao, C. and Chen, Y.-G. (2010). Dishevelled: the hub of Wnt signaling. *Cell. Signal.* **22**, 717-727. doi:10.1016/j.cellsig.2009.11.021

Gray, R. S., Bayly, R. D., Green, S. A., Agarwala, S., Lowe, C. J. and Wallingford, J. B. (2009). Diversification of the expression patterns and developmental functions of the dishevelled gene family during chordate evolution. *Dev. Dyn.* **238**, 2044-2057. doi:10.1002/dvdy.22028

Habas, R., Dawid, I. B. and He, X. (2003). Coactivation of Rac and Rho by Wnt/Frizzled signaling is required for vertebrate gastrulation. *Genes Dev.* **17**, 295-309. doi:10.1101/gad.1022203

Hall, A. (1998). Rho GTPases and the actin cytoskeleton. *Science* **279**, 509-514. doi:10.1126/science.279.5350.509

Harland, R. M. (1991). In situ hybridization: an improved whole-mount method for Xenopus embryos. *Methods Cell Biol.* **36**, 685-695. doi:10.1016/s0091-679x(08)60307-6

Itoh, K., Antipova, A., Ratcliffe, M. J. and Sokol, S. (2000). Interaction of dishevelled and Xenopus axin-related protein is required for wnt signal transduction. *Mol. Cell. Biol.* **20**, 2228-2238. doi:10.1128/MCB.20.6.2228-2238.2000

Jaffe, A. B. and Hall, A. (2005). Rho GTPases: biochemistry and biology. *Annu. Rev. Cell Dev. Biol.* **21**, 247-269. doi:10.1146/annurev.cellbio.21.020604.150721

Kashef, J., Kohler, A., Kuriyama, S., Alfandari, D., Mayor, R. and Wedlich, D. (2009). Cadherin-11 regulates protrusive activity in Xenopus cranial neural crest cells upstream of Trio and the small GTPases. *Genes Dev.* **23**, 1393-1398. doi:10.1101/gad.519409

Kratzer, M.-C., England, L., Apel, D., Hassel, M. and Borchers, A. (2019). Evolution of the Rho guanine nucleotide exchange factors Kalirin and Trio and their gene expression in Xenopus development. *Gene Expr. Patterns* **32**, 18-27. doi:10.1016/j.gep.2019.02.004

Landin Malt, A., Dailey, Z., Holbrook-Rasmussen, J., Zheng, Y., Hogan, A., Du, Q. and Lu, X. (2019). Par3 is essential for the establishment of planar cell polarity of inner ear hair cells. *Proc. Natl. Acad. Sci. USA* **116**, 4999-5008. doi:10.1073/pnas.1816333116

Langhe, R. P., Gudzenko, T., Bachmann, M., Becker, S. F., Gonnermann, C., Winter, C., Abbruzzese, G., Alfandari, D., Kratzer, M.-C., Franz, C. M. et al. (2016). Cadherin-11 localizes to focal adhesions and promotes cell-substrate adhesion. *Nat. Commun.* **7**, 10909. doi:10.1038/ncomms10909

Li, Y., Guo, Z., Chen, H., Dong, Z., Pan, Z. K., Ding, H., Su, S.-B. and Huang, S. (2011). HOXC8-dependent cadherin 11 expression facilitates breast cancer cell migration through Trio and Rac. *Genes Cancer* **2**, 880-888. doi:10.1177/1947601911433129

Luo, T., Lee, Y.-H., Saint-Jeannet, J.-P. and Sargent, T. D. (2003). Induction of neural crest in Xenopus by transcription factor AP2alpha. *Proc. Natl. Acad. Sci. USA* **100**, 532-537. doi:10.1073/pnas.0237226100

Matthews, H. K., Marchant, L., Carmona-Fontaine, C., Kuriyama, S., Larrain, J., Holt, M. R., Parsons, M. and Mayor, R. (2008). Directional migration of neural crest cells in vivo is regulated by Syndecan-4/Rac1 and non-canonical Wnt signaling/RhoA. *Development* **135**, 1771-1780. doi:10.1242/dev.017350

McLennan, R., Teddy, J. M., Kasemeier-Kulesa, J. C., Romine, M. H. and Kulesa, P. M. (2010). Vascular endothelial growth factor (VEGF) regulates cranial neural crest migration in vivo. *Dev. Biol.* **339**, 114-125. doi:10.1016/j.ydbio.2009.12.022

Medina, A. and Steinbeisser, H. (2000). Interaction of Frizzled 7 and dishevelled in Xenopus. *Dev. Dyn.* **218**, 671-680. doi:10.1002/1097-0177(2000)9999:9999<::AID-DVDY1017>3.0.CO;2-9

Medina, A., Reintsch, W. and Steinbeisser, H. (2000). Xenopus frizzled 7 can act in canonical and non-canonical Wnt signaling pathways: implications on early patterning and morphogenesis. *Mech. Dev.* **92**, 227-237. doi:10.1016/S0925-4773(00)00240-9

Medley, Q. G., Buchbinder, E. G., Tachibana, K., Ngo, H., Serra-Pagès, C. and Streuli, M. (2003). Signaling between focal adhesion kinase and trio. *J. Biol. Chem.* **278**, 13265-13270. doi:10.1074/jbc.M300277200

Miller, J. R., Rowning, B. A., Larabell, C. A., Yang-Snyder, J. A., Bates, R. L. and Moon, R. T. (1999). Establishment of the dorsal-ventral axis in Xenopus embryos coincides with the dorsal enrichment of dishevelled that is dependent on cortical rotation. *J. Cell Biol.* **146**, 427-437. doi:10.1083/jcb.146.2.427

Moore, R., Theveneau, E., Pozzi, S., Alexandre, P., Richardson, J., Merks, A., Parsons, M., Kashef, J., Linker, C. and Mayor, R. (2013). Par3 controls neural crest migration by promoting microtubule catastrophe during contact inhibition of locomotion. *Development* **140**, 4763-4775. doi:10.1242/dev.098509

Moriyoshi, K., Richards, L. J., Akazawa, C., O'Leary, D. D. M. and Nakanishi, S. (1996). Labeling neural cells using adenoviral gene transfer of membrane-targeted GFP. *Neuron* **16**, 255-260. doi:10.1016/S0896-6273(00)80044-6

Narimatsu, M., Bose, R., Pye, M., Zhang, L., Miller, B., Ching, P., Sakuma, R., Luga, V., Roncari, L., Attisano, L. et al. (2009). Regulation of planar cell polarity by Smurf ubiquitin ligases. *Cell* **137**, 295-307. doi:10.1016/j.cell.2009.02.025

Nguyen, L. K., Kholodenko, B. N. and von Kriegsheim, A. (2018). Rac1 and RhoA: networks, loops and bistability. *Small GTPases* **9**, 316-321. doi:10.1080/21541248.2016.1224399

Nieuwkoop, P. D. and Faber, J. (1967). *Normal Table of Xenopus laevis (Daudin)*, 2nd edn. Amsterdam: North Holland.

Paclikova, P., Bernatik, O., Radaszkiewicz, T. W. and Bryja, V. (2017). The N-terminal part of the dishevelled DEP domain is required for Wnt/beta-catenin signaling in mammalian cells. *Mol. Cell. Biol.* **37**, e00145-17. doi:10.1128/MCB.00145-17

Pengelly, R. J., Greville-Heygate, S., Schmidt, S., Seaby, E. G., Jabalameli, M. R., Mehta, S. G., Parker, M. J., Goudie, D., Fagotto-Kaufmann, C., Mercer, C. et al. (2016). Mutations specific to the Rac-GEF domain of TRIO cause intellectual disability and microcephaly. *J. Med. Genet.* **53**, 735-742. doi:10.1136/jmedgenet-2016-103942

Ren, X.-D., Kiosses, W. B. and Schwartz, M. A. (1999). Regulation of the small GTP-binding protein Rho by cell adhesion and the cytoskeleton. *EMBO J.* **18**, 578-585. doi:10.1093/emboj/18.3.578

Riedl, J., Crevenna, A. H., Kessenbrock, K., Yu, J. H., Neukirchen, D., Bista, M., Bradke, F., Jenne, D., Holak, T. A., Werb, Z. et al. (2008). Lifeact: a versatile marker to visualize F-actin. *Nat. Methods* **5**, 605-607. doi:10.1038/nmeth.1220

Rothbächer, U., Laurent, M. N., Deardorff, M. A., Klein, P. S., Cho, K. W. Y. and Fraser, S. E. (2000). Dishevelled phosphorylation, subcellular localization and multimerization regulate its role in early embryogenesis. *EMBO J.* **19**, 1010-1022. doi:10.1093/emboj/19.5.1010

Roycroft, A. and Mayor, R. (2018). Michael Abercrombie: contact inhibition of locomotion and more. *Int. J. Dev. Biol.* **62**, 5-13. doi:10.1387/ijdb.170277rm

Schambony, A. and Wedlich, D. (2007). Wnt-5A/Ror2 regulate expression of XPAPC through an alternative noncanonical signaling pathway. *Dev. Cell* **12**, 779-792. doi:10.1016/j.devcel.2007.02.016

Schmidt, S. and Debant, A. (2014). Function and regulation of the Rho guanine nucleotide exchange factor Trio. *Small GTPases* **5**, e29769. doi:10.4161/sgtp.29769

Schwarz-Romond, T., Merrifield, C., Nichols, B. J. and Bienz, M. (2005). The Wnt signalling effector Dishevelled forms dynamic protein assemblies rather than stable associations with cytoplasmic vesicles. *J. Cell Sci.* **118**, 5269-5277. doi:10.1242/jcs.02646

Sheldahl, L. C., Slusarski, D. C., Pandur, P., Miller, J. R., Kuhl, M. and Moon, R. T. (2003). Dishevelled activates Ca2+ flux, PKC, and CamKII in vertebrate embryos. *J. Cell Biol.* **161**, 769-777. doi:10.1083/jcb.200211094

Shellard, A. and Mayor, R. (2016). Chemotaxis during neural crest migration. *Semin. Cell Dev. Biol.* **55**, 111-118. doi:10.1016/j.semcdb.2016.01.031

Smalley, M. J., Signoret, N., Robertson, D., Tilley, A., Hann, A., Ewan, K., Ding, Y., Paterson, H. and Dale, T. C. (2005). Dishevelled (Dvl-2) activates canonical Wnt signalling in the absence of cytoplasmic puncta. *J. Cell Sci.* **118**, 5279-5289. doi:10.1242/jcs.02647

Smith, A., Robinson, V., Patel, K. and Wilkinson, D. G. (1997). The EphA4 and EphB1 receptor tyrosine kinases and ephrin-B2 ligand regulate targeted migration of branchial neural crest cells. *Curr. Biol.* **7**, 561-570. doi:10.1016/S0960-9822(06)00255-7

Sokol, S. Y. (1996). Analysis of Dishevelled signalling pathways during Xenopus development. *Curr. Biol.* **6**, 1456-1467. doi:10.1016/S0960-9822(96)00750-6

Szabó, A. and Mayor, R. (2018). Mechanisms of neural crest migration. *Annu. Rev. Genet.* **52**, 43-63. doi:10.1146/annurev-genet-120417-031559

Theveneau, E. and Mayor, R. (2011). Collective cell migration of the cephalic neural crest: the art of integrating information. *Genesis* **49**, 164-176. doi:10.1002/dvg.20700

Theveneau, E., Marchant, L., Kuriyama, S., Gull, M., Moepps, B., Parsons, M. and Mayor, R. (2010). Collective chemotaxis requires contact-dependent cell polarity. *Dev. Cell* **19**, 39-53. doi:10.1016/j.devcel.2010.06.012

Theveneau, E., Steventon, B., Scarpa, E., Garcia, S., Trepat, X., Streit, A. and Mayor, R. (2013). Chase-and-run between adjacent cell populations promotes directional collective migration. *Nat. Cell Biol.* **15**, 763-772. doi:10.1038/ncb2772

Timmerman, I., Heemskerk, N., Kroon, J., Schaefer, A., van Rijssel, J., Hoogenboezem, M., van Unen, J., Goedhart, J., Gadella, T. W. J., Jr., Yin, T. et al. (2015). A local VE-cadherin and Trio-based signaling complex stabilizes endothelial junctions through Rac1. *J. Cell Sci.* **128**, 3514. doi:10.1242/jcs.179424

Trainor, P. A. (2014). *Neural Crest Cells: Evolution, Development, and Disease*. Amsterdam; Boston: Elsevier/AP, Academic Press is an imprint of Elsevier.

DEVELOPMENT

van Rijssel, J. and van Buul, J. D. (2012). The many faces of the guanine-nucleotide exchange factor trio. *Cell Adh Migr* **6**, 482-487. doi:10.4161/cam.21418

Vanderzalm, P. J., Pandey, A., Hurwitz, M. E., Bloom, L., Horvitz, H. R. and Garriga, G. (2009). C. elegans CARMIL negatively regulates UNC-73/Trio function during neuronal development. *Development* **136**, 1201-1210. doi:10.1242/dev.026666

Wallingford, J. B. and Habas, R. (2005). The developmental biology of Dishevelled: an enigmatic protein governing cell fate and cell polarity. *Development* **132**, 4421-4436. doi:10.1242/dev.02068

Winklbauer, R., Medina, A., Swain, R. K. and Steinbeisser, H. (2001). Frizzled-7 signalling controls tissue separation during Xenopus gastrulation. *Nature* **413**, 856-860. doi:10.1038/35101621

Yang-Snyder, J., Miller, J. R., Brown, J. D., Lai, C.-J. and Moon, R. T. (1996). A frizzled homolog functions in a vertebrate Wnt signaling pathway. *Curr. Biol.* **6**, 1302-1306. doi:10.1016/S0960-9822(02)70716-1

Yano, T., Yamazaki, Y., Adachi, M., Okawa, K., Fort, P., Uji, M. and Tsukita, S. (2011). Tara up-regulates E-cadherin transcription by binding to the Trio RhoGEF and inhibiting Rac signaling. *J. Cell Biol.* **193**, 319-332. doi:10.1083/jcb.201009100

DEVELOPMENT